Mixing effects of $\eta - \eta'$ in $\Lambda_b \to \Lambda\eta^{(')}$ decays

Zhou Rui[ORCID],[*] Jia-Ming Li, and Chao-Qi Zhang[ORCID]

College of Sciences, North China University of Science and Technology, Tangshan 063009, China

We perform a thorough analysis of the $\eta - \eta'$ mixing effects on the $\Lambda_b \to \Lambda\eta^{(')}$ decays based on the perturbative QCD (PQCD) factorization approach. Branching ratios, up-down asymmetries, and direct CP asymmetries are computed by considering four popular mixing schemes, such as $\eta - \eta'$, $\eta - \eta' - \eta_c$, $\eta - \eta' - G$, and $\eta - \eta' - G - \eta_c$ mixing formalisms, where G represents the physical pseudoscalar glueball. The PQCD predictions with the four mixing schemes does not change much for the η channel but changes significantly for the η' one. In particular, the value of $\mathcal{B}(\Lambda_b \to \Lambda\eta')$ in the $\eta - \eta' - G - \eta_c$ mixing scheme exceeds the present experimental bound by a factor of 2, indicating the related mixing angles may be overestimated. Because of the distinctive patterns of interference between S-wave and P-wave amplitudes, the predicted up-down asymmetries for the two modes differ significantly. The obvious discrepancies among different theoretical analyses should be clarified in the future. The direct CP violations are predicted to be at the level of a few percent mainly because the tree contributions of the strange and nonstrange amplitudes suffer from the color suppression and CKM suppression. Finally, as a by-product, we investigate the $\Lambda_b \to \Lambda\eta_c$ process, which has a large branching ratio of order 10^{-4}, promising to be measured by the LHCb experiment. Our findings are useful for constraining the mixing parameters, comprehending the $\eta^{(')}$ configurations, and instructing experimental measurements.

I. INTRODUCTION

The phenomenon of mixing in the $\eta - \eta'$ system is an interesting subject in hadron physics. In the exact $SU(3)$ flavor-symmetry limit, the pseudoscalar meson η would be a pure flavor octet and η' a flavor singlet. However, it is known that the $SU(3)$ flavor symmetry breaking will lead to $\eta - \eta'$ mixing, which can be either described in the octet-singlet basis [1,2] or in the quark-flavor basis [3,4]. Occasionally, allowing for the heavier charm component in the η and η' mesons [5,6], one has to consider the $c\bar{c}$ components in the mixing basis. In the QCD case, apart from the quark-antiquark combinations, pure gluon configurations, such as the two-gluon states, can also form an $SU(3)$ singlet, which allows a possible gluonic admixture in η' mesons [7–14]. The $\eta - \eta'$ mixing phenomenon could then be generalized to include more states, such as glueballs and η_c mesons [15,16]. In this respect, a better knowledge of the quark and gluon components inside the η and η' states deepens our understanding of nonperturbative QCD

dynamics in flavor physics [17], and the beauty hadron decays to η, η' pseudoscalar mesons can be used to shed light on these phenomena.

In the B meson sector, the observed hierarchy of $\mathcal{B}(B \to \eta'K) \gg \mathcal{B}(B \to \eta K)$ [18] has attracted much attention, and many solutions have been proposed [10,19–24]. The large difference suggests a contribution to $\mathcal{B}(B \to \eta'K)$ via the $SU(3)$ singlet component of the η and η'. It has been known that the gluonic and charm contents of the light pseudoscalar mesons η and η' may have a crucial impact on studies of many hadronic processes [17]. Various mixing mechanisms in $B \to \eta^{(')}$ decays have been explored in the context of perturbative QCD factorization (PQCD), in which the transverse momenta of valence quarks are included to regulate the end-point singularities; see, e.g., Refs. [6,25–29]. The earlier PQCD predictions at leading order for $B \to \eta^{(')}K$ without the flavor-singlet amplitudes are higher (lower) than the measured values [28]. Although the partial next-to-leading order (NLO) contributions are included in [25], the gap between theory and experiment is still not completely understood. In Ref. [27], the authors examined the gluonic contribution to the $B \to \eta, \eta'$ transition form factors and found that it is numerically neglected. A mixing scheme for η, η', and the pseudoscalar glueball was proposed in [30], in which the formalism for the $\eta - \eta' - G$ mixing was set up. Three years later, this trimixing formalism was further extended to the $\eta - \eta' - G - \eta_c$ tetramixing by including the η_c meson in Ref. [6]. They discovered that the η_c-mixing effects enhance the PQCD

[*]Corresponding author.
jindui1127@126.com

predictions for $\mathcal{B}(B \to \eta' K)$ by 18% but not for $\mathcal{B}(B \to \eta K)$, and they claimed that the puzzle of the above distinctive pattern can be resolved. In Ref. [26], three different mixing schemes for the $\eta - \eta'$ system were taken into account, and the PQCD calculations for the $B \to \eta^{(')} K$ decays were improved to the NLO level. It is found that the NLO PQCD predictions in the $\eta - \eta' - G$ mixing scheme provide a nearly perfect interpretation of the measured values.

The $\eta - \eta' - G$ mixing scheme was also applied to the $B \to J/\psi \eta^{(')}$ decays [31] in PQCD. A large gluon contribution was advocated from the analysis of relative probabilities of the $B_s \to J/\psi \eta'$ and $B_s \to J/\psi \eta$ decays. However, the subsequent measurements from LHCb [32,33] hint at a small gluonic component in the η' meson. It is then worthwhile to examine whether these mixing schemes can explain the measurements well in the baryon reactions involving η or η' mesons, such as $\Lambda_b \to \Lambda \eta^{(')}$ decays.

Searches for the $\Lambda_b \to \Lambda \eta$ and $\Lambda_b \to \Lambda \eta'$ decays have been performed by the LHCb [34] Collaboration. The branching ratio of the former was measured to be $\mathcal{B}(\Lambda_b \to \Lambda \eta) = 9.3^{+7.3}_{-5.3} \times 10^{-6}$ at the level of 3σ significance, while an upper limit for the latter mode was set as 3.1×10^{-6} at the 90% confidence level. Some predictions exist for the $\Lambda_b \to \Lambda \eta^{(')}$ decays. Within the framework of the light-front quark model (LFQM) [35], the branching ratios were estimated to be at the order of 10^{-8} in the absence of penguin contributions. In Ref. [36], based on the QCD factorization (QCDF), the branching ratios were predicted to be in the ranges $\mathcal{B}(\Lambda_b \to \Lambda \eta) \sim (3-6) \times 10^{-7}$ and $\mathcal{B}(\Lambda_b \to \Lambda \eta') \sim (3-7) \times 10^{-6}$ with large theoretical uncertainties, while in Ref. [37] the branching ratios were calculated to be $\mathcal{B}(\Lambda_b \to \Lambda \eta, \Lambda \eta') = (1.47 \pm 0.35, 1.83 \pm 0.58) \times 10^{-6}$, exploiting the generalized factorization approach (GFA). In an earlier paper [38], a wider range, $(1.8 - 19.0) \times 10^{-6}$, was estimated by using different models for the $\Lambda_b \to \Lambda$ form factors.

Our purpose in the present paper is to probe the $\eta - \eta'$ mixing in the $\Lambda_b \to \Lambda \eta^{(')}$ decays by employing the PQCD approach at leading order accuracy. Four available mixing schemes for the $\eta - \eta'$ system—namely, $\eta - \eta'$, $\eta - \eta' - G$, $\eta - \eta' - G - \eta_c$, and $\eta - \eta' - \eta_c$ mixing—are taken into account. The effect of radial mixing is neglected due to the absence of $\Lambda_b \to \eta^{(')}$ form factors in the relevant processes [39], and the mixing with the pion under the isospin symmetry is not considered either. Within these mixing schemes, we calculate the branching ratios, up-down asymmetries, and direct CP violations for $\Lambda_b \to \Lambda \eta^{(')}$ and investigate the scheme dependence of the theoretical predictions.

The paper is organized as follows. In Sec. II, we first discuss the four mixing schemes as well as the related mixing angles and review the hadronic light-cone distribution amplitudes (LCDAs). Then, we briefly present the

effective Hamiltonian and kinematics for the PQCD calculations. We show the PQCD predictions for the branching ratios, up-down asymmetries, and direct CP asymmetries of the relevant decays with four different mixing schemes in Sec. III. A summary will be given in the last section. The Appendix is devoted to details for the computation of the decay amplitudes within PQCD.

II. THEORETICAL FRAMEWORK

A. $\eta - \eta'$ mixing phenomenon

This section is devoted to the phenomenological aspects of $\eta - \eta'$ mixing. In this work we consistently use the quark-flavor mixing basis rather than the singlet-octet mixing basis since fewer two-parton twist-3 meson distribution amplitudes need to be introduced [27]. Following the analysis of Refs. [3,6,26,30], we first introduce four different $\eta - \eta'$ mixing schemes. In the conventional Feldmann-Kroll-Stech (FKS) scheme [3,4] for the $\eta - \eta'$ mixing, the physical neutral pseudoscalar mesons $\eta^{(')}$ can be represented as a superposition of isosinglet states,

$$\begin{pmatrix} \eta \\ \eta' \end{pmatrix} = \begin{pmatrix} c\phi & -s\phi \\ s\phi & c\phi \end{pmatrix} \begin{pmatrix} \eta_q \\ \eta_s \end{pmatrix}, \tag{1}$$

with shorthand $(c, s) \equiv (\cos, \sin)$ and ϕ being the mixing angle. Here, $\eta_q = (u\bar{u} + d\bar{d})/\sqrt{2}$ and $\eta_s = s\bar{s}$ are the so-called nonstrange and strange quark-flavor states, respectively. The presence of only one mixing angle in this case is due to the Okubo-Zweig-Iizuka (OZI) suppressed contributions being neglected [15]. For details of the two-angle mixing scheme for the $\eta - \eta'$ system, see Refs. [40,41].

Alternatively, allowing for another heavy-quark charm $c\bar{c}$ component in the η and η', the conventional FKS formalism can be generalized naturally to the trimixing of $\eta - \eta' - \eta_c$ in the $q\bar{q} - s\bar{s} - c\bar{c}$ basis. The physical states are related to the flavor states via [3]

$$\begin{pmatrix} \eta \\ \eta' \\ \eta_c \end{pmatrix} = \begin{pmatrix} c\phi & -s\phi & -\theta_c s\theta_y \\ s\phi & c\phi & \theta_c c\theta_y \\ -\theta_c s(\phi - \theta_y) & -\theta_c c(\phi - \theta_y) & 1 \end{pmatrix} \begin{pmatrix} \eta_q \\ \eta_s \\ \eta_c \end{pmatrix}, \tag{2}$$

where θ_c and θ_y are two new mixing angles related to the charm decay constants of the $\eta^{(')}$ mesons.

In QCD, gluons may form a bound state, called gluonium, that can mix with neutral mesons [11]. By including a possible pseudoscalar glueball state η_g in the $\eta^{(')}$ mesons [14,30], the FKS mixing scheme can be extended to the $\eta - \eta' - G$ mixing formalism, where G denotes the physical pseudoscalar glueball. Using the quark-flavor basis, we can write [30,31]

$$
\begin{pmatrix} \eta \\ \eta' \\ G \end{pmatrix} = \begin{pmatrix} c\phi + s\theta s\theta_i(1 - c\phi_G) & -s\phi + s\theta c\theta_i(1 - c\phi_G) & -s\theta s\phi_G \\ s\phi - c\theta s\theta_i(1 - c\phi_G) & c\phi - c\theta c\theta_i(1 - c\phi_G) & c\theta s\phi_G \\ -s\theta_i s\phi_G & -c\theta_i s\phi_G & c\phi_G \end{pmatrix} \begin{pmatrix} \eta_q \\ \eta_s \\ \eta_g \end{pmatrix}, \tag{3}
$$

where $\theta_i = 54.7°$ is the ideal mixing angle between the octet-singlet and the quark-flavor states in the SU(3) flavor-symmetry limit [17,42]. Here, θ is related to ϕ by $\theta = \phi - \theta_i$, and ϕ_G is the mixing angle for the gluonium contribution. We assume that the glueball only mixes with the flavor-singlet η_1 but not with the flavor-octet η_8, so the two mixing angles ϕ and ϕ_G are sufficient to describe the mixing matrix in Eq. (3). It has been verified that the contribution from the gluonic distribution amplitudes in the $\eta^{(')}$ meson is negligible for B meson transition form factors [27]. Hence, we still suppose that the η and η' mesons are produced via the nonstrange (strange) component in the baryon decays under the $\eta - \eta' - G$ mixing.

In [6], the authors combined the above two trimixings by considering the tetramixing of $\eta - \eta' - G - \eta_c$, which is described by a 4×4 mixing matrix. It was assumed that the heavy-flavor state only mixes with the pseudoscalar glueball; then the transformation reads

$$
\begin{pmatrix} \eta \\ \eta' \\ G \\ \eta_c \end{pmatrix} = \begin{pmatrix} c\theta c\theta_i - s\theta s\theta_i c\phi_G & -c\theta s\theta_i - s\theta c\theta_i c\phi_G & -s\theta s\phi_G c\phi_C & -s\theta s\phi_G s\phi_C \\ s\theta c\theta_i + c\theta s\theta_i c\phi_G & -s\theta s\theta_i + c\theta c\theta_i c\phi_G & c\theta s\phi_G c\phi_C & c\theta s\phi_G s\phi_C \\ s\theta_i s\phi_G & -c\theta_i s\phi_G & c\phi_G c\phi_C & c\phi_G s\phi_C \\ 0 & 0 & -s\phi_C & c\phi_C \end{pmatrix} \begin{pmatrix} \eta_q \\ \eta_s \\ \eta_g \\ \eta_c \end{pmatrix}, \tag{4}
$$

where the new angle ϕ_C is the mixing angle between the glueball and η_c components. It can be easily seen that the $\eta - \eta' - G - \eta_c$ tetramixing formalism reduces to the $\eta - \eta' - G$ and FKS schemes in the $\phi_C \to 0$ and $\phi_{C,G} \to 0$ limits, respectively.

As the mixing of η and η' is still not completely clear at the moment, they may be mixed with the radial excitations, leading to more complicated mixing formalism. In the following analysis, we ignore other possible admixtures from radial excitations. In addition, we assume that isospin symmetry is exact ($m_u = m_d \ll m_s$); the mixing with π—such as the $\pi - \eta$ mixing [43], the trimixing of $\pi - \eta - \eta'$ [44,45], and the tetramixing of $\pi - \eta - \eta' - \eta_c$ [46]—are not considered here.

B. Light-cone distribution amplitudes

The hadronic LCDAs are important in PQCD calculations, which describe the momentum fraction distribution of valence quarks inside hadrons. There are various models of the Λ_b and Λ baryon LCDAs available in the literature [47–58]. In this work, we adopt the exponential model LCDAs for the Λ_b baryon [49] and Chernyak-Ogloblin-Zhitnitsky (COZ) model for the Λ [53], whose explicit expressions can be found in the previous work [59–61] and shall not be repeated here. It has been confirmed that the models employed lead to reasonable numerical results for the $\Lambda_b \to \Lambda$ form factor with fewer free parameters [59].

Two-parton quark components for the $\eta_{s,c}$ mesons are defined via the nonlocal matrix elements [27,62,63]

$$
\langle \eta_s(q)|\bar{s}_\beta(z)s_\alpha(0)|0\rangle = -\frac{i}{\sqrt{2N_c}} \int_0^1 dy e^{iyq\cdot z}\gamma_5[\slashed{q}\phi_s^A(y) + m_0^s\phi_s^P(y) + m_0^s(\slashed{n}\slashed{v} - 1)\phi_s^T(y)]_{\alpha\beta},
$$

$$
\langle \eta_c(q)|\bar{c}_\beta(z)c_\alpha(0)|0\rangle = -\frac{i}{\sqrt{2N_c}} \int_0^1 dy e^{iyq\cdot z}\gamma_5[\slashed{q}\phi_{\eta_c}^v(y) + m_{\eta_c}\phi_{\eta_c}^s(y)], \tag{5}
$$

where N_c is the number of colors. Here, η_q can be obtained by substituting s for d in Eq. (5) and multiplying by a factor of $1/\sqrt{2}$. The two light-cone vectors $n = (1, 0, \mathbf{0}_T)$ and $v = (0, 1, \mathbf{0}_T)$ satisfy $n \cdot v = 1$. Note that $m_0^{q,s}$ are the chiral enhancement scales associated with the twist-3 LCDAs, which can be expressed in terms of the decay constants $f_{q,s}$ and the mixing angles. Their values can be fixed by solving for the mass matrix in different mixing schemes [3], which will be given in the next section.

The models for the various twist distribution amplitudes have been determined in [64,65],

$$\phi_{q,s}^A(y) = \frac{f_{q,s}}{2\sqrt{2N_c}} 6y(1-y)[1 + a_2 C_2^{3/2}(u) + a_4 C_4^{3/2}(u)],$$

$$\phi_{q,s}^P(y) = \frac{f_{q,s}}{2\sqrt{2N_c}}\left[1 + \left(30\eta_3 - \frac{5}{2}\rho_{q,s}^2\right)C_2^{1/2}(u) - 3\left(\eta_3\omega_3 + \frac{9}{20}\rho_{q,s}^2(1 + 6a_2)\right)C_4^{1/2}(u)\right],$$

$$\phi_{q,s}^T(y) = \frac{f_{q,s}}{2\sqrt{2N_c}}(1-2y)\left[1 + 6\left(5\eta_3 - \frac{1}{2}\eta_3\omega_3 - \frac{7}{20}\rho_{q,s}^2 - \frac{3}{5}\rho_{q,s}^2 a_2\right)(1 - 10y + 10y^2)\right],$$

$$\phi_{\eta_c}^v(y,b) = \frac{f_{\eta_c}}{2\sqrt{2N_c}}N^v y(1-y)\exp\left\{-\frac{m_c}{\omega}y(1-y)\left[\left(\frac{1-2y}{2y(1-y)}\right)^2 + \omega^2 b^2\right]\right\},$$

$$\phi_{\eta_c}^s(y,b) = \frac{f_{\eta_c}}{2\sqrt{2N_c}}N^s \exp\left\{-\frac{m_c}{\omega}y(1-y)\left[\left(\frac{1-2y}{2y(1-y)}\right)^2 + \omega^2 b^2\right]\right\}, \tag{6}$$

where we resort to SU(3) symmetry and use the same Gegenbauer moments for the η_q and η_s. This approximation is reasonable since the main SU(3) breaking in Gegenbauer moments is due to the nonzero odd terms and that in a_2 is subleading [66]. Here, we include the SU(3)-breaking effect via the decay constants, the chiral scales, and the parameters $\rho_{q,s}$ in the LCDAs. These nonperturbative parameters are not all independent. The two mass ratios $\rho_{q,s}$ are related to the respective chiral scales by $\rho_{q,s} = 2m_{q,s}/m_0^{q,s}$, with $m_{q,s}$ being the current quark masses. The two parameters $\eta_3 = 0.015$ and $\omega_3 = -3$ are the same as for the pion distribution amplitudes [64]. The Gegenbauer polynomials $C(u)$ are given as

$$C_2^{3/2}(u) = \frac{3}{2}(5u^2 - 1), \qquad C_2^{1/2}(u) = \frac{1}{2}(3u^2 - 1),$$

$$C_4^{1/2}(u) = \frac{1}{8}(3 - 30u^2 + 35u^4),$$

$$C_4^{3/2}(u) = \frac{15}{8}(1 - 14u^2 + 21u^4), \tag{7}$$

with $u = 2y - 1$. The shape parameter $\omega = 0.6$ GeV is taken from [65]. Note that f_{η_c} and m_{η_c} are the decay constant and mass of the η_c meson, respectively. The two normalization constants $N^{v,s}$ are determined by [65]

$$\int_0^1 dy\,\phi_{\eta_c}^{v,s}(y, b = 0) = \frac{f_{\eta_c}}{2\sqrt{2N_c}}. \tag{8}$$

C. PQCD calculation

The PQCD approach has been developed and successfully applied to deal with the Λ_b hadronic decays [59–61,67–73]. In the PQCD picture, the decay amplitudes can be calculated by the convolution of the nonperturbative,

universal LCDAs and the perturbative hard scattering amplitude. After defining the nonperturbative LCDAs in the last subsection, we are ready to calculate the decay amplitudes of the strong coupling constant at leading order. Various topological diagrams responsible for the considered decays are presented in Fig. 1. The labels T, C, E, and B refer to external W emission, internal W emission, W exchange, and bow-tie topologies, respectively. The subscript $q(s)$ of E corresponds to the contribution from the nonstrange (strange) component in the $\eta^{(\prime)}$ mesons. Exchanging two identical quarks in the final-state baryon and meson for the E- or B-type diagram, we obtain a new topology denoted by B' as exhibited in the last diagram of Fig. 1. We draw one representative Feynman diagram for each topology here; for a more complete set of Feynman diagrams, refer to our previous work [59,60,73].

In the Λ_b rest frame, we choose the $\Lambda_b(\Lambda)$ baryon momentum $p(p')$ and the meson momentum q in the light-cone coordinates:

$$p = \frac{M}{\sqrt{2}}(1, 1, \mathbf{0}_T), \qquad p' = \frac{M}{\sqrt{2}}(f^+, f^-, \mathbf{0}_T),$$

$$q = \frac{M}{\sqrt{2}}(1 - f^+, 1 - f^-, \mathbf{0}_T), \tag{9}$$

with M being the Λ_b baryon mass. The factors $f^{\pm}$ can be derived from the on-shell conditions $p'^2 = m_\Lambda^2$ and $q^2 = m^2$ for the final-state hadrons, which yield

$$f^{\pm} = \frac{1}{2}\left(1 - r^2 + r_\Lambda^2 \pm \sqrt{(1 - r^2 + r_\Lambda^2)^2 - 4r_\Lambda^2}\right), \tag{10}$$

with the mass ratios $r_{(\Lambda)} = m_{(\Lambda)}/M$. The spectator momenta inside the initial and final states are parametrized as
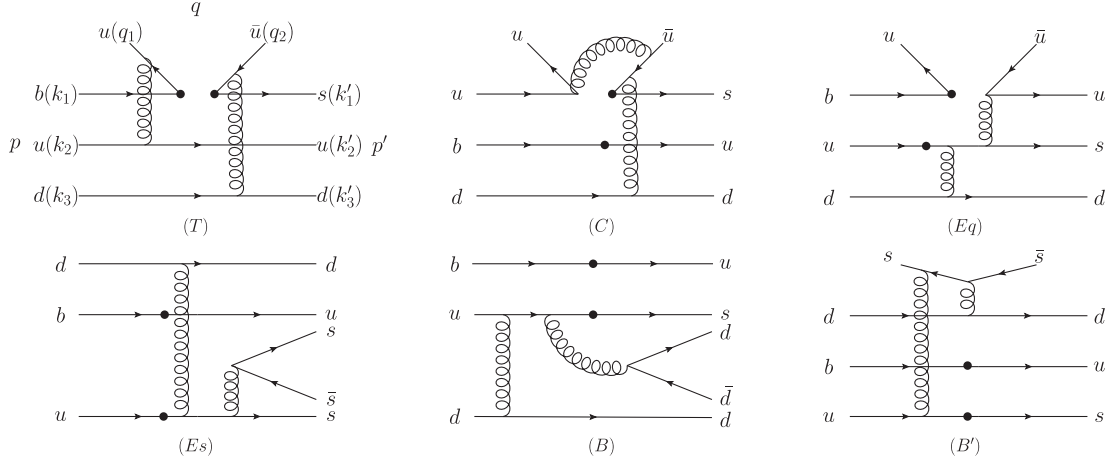
FIG. 1.   Sample topological diagrams responsible for the decay $\Lambda_b \to \Lambda \eta^{(\prime)}$. Here, T denotes the external W emission diagram, C represents the internal W emission diagram, $E_{q(s)}$ labels the W exchange diagram with nonstrange (strange) components contributing to the $\eta^{(\prime)}$ mesons, B denotes the bow-tie-type W exchange diagram, and B' represents the diagram that can be obtained from the W exchange diagram by exchanging the two identical quarks in the final states.

$$k_1 = \left(\frac{M}{\sqrt{2}}, \frac{M}{\sqrt{2}}x_1, \mathbf{k}_{1T}\right), \qquad k_2 = \left(0, \frac{M}{\sqrt{2}}x_2, \mathbf{k}_{2T}\right), \qquad k_3 = \left(0, \frac{M}{\sqrt{2}}x_3, \mathbf{k}_{3T}\right),$$

$$k_1' = \left(\frac{M}{\sqrt{2}}f^+ x_1', 0, \mathbf{k}_{1T}'\right), \qquad k_2' = \left(\frac{M}{\sqrt{2}}f^+ x_2', 0, \mathbf{k}_{2T}'\right), \qquad k_3' = \left(\frac{M}{\sqrt{2}}f^+ x_3', 0, \mathbf{k}_{3T}'\right),$$

$$q_1 = \left(\frac{M}{\sqrt{2}}y(1-f^+), \frac{M}{\sqrt{2}}y(1-f^-), \mathbf{q}_T\right),$$

$$q_2 = \left(\frac{M}{\sqrt{2}}(1-y)(1-f^+), \frac{M}{\sqrt{2}}(1-y)(1-f^-), -\mathbf{q}_T\right), \tag{11}$$

where $x_{1,2,3}^{(\prime)}$ and y are the parton longitudinal momentum fractions, and $\mathbf{k}_{1T,2T,3T}^{(\prime)}$ and $\mathbf{q}_T$ are the corresponding transverse momenta. The momentum conservation implies the relations

$$\sum_{l=1}^{3} x_l^{(\prime)} = 1, \qquad \sum_{l=1}^{3} \mathbf{k}_{lT}^{(\prime)} = 0. \tag{12}$$

Here, all the kinematical variables are labeled in the first diagram of Fig. 1.

Based on the operator product expansion, the effective weak-interaction Hamiltonian for the $b \to s$ transition reads [74]

$$\mathcal{H}_{\text{eff}} = \frac{G_F}{\sqrt{2}} \left\{ V_{Qb} V_{Qs}^* [C_1(\mu) O_1^Q(\mu) + C_2(\mu) O_2^Q(\mu)] - \sum_k V_{tb} V_{ts}^* C_k(\mu) O_k(\mu) \right\} + \text{H.c.}, \tag{13}$$

where $V_{Qb,Qs,tb,ts}$ are the Cabibbo-Kobayashi-Maskawa (CKM) matrix elements with $Q = u$ for $\eta_{q,s}$ and $Q = c$ for η_c. Here, G_F is the Fermi constant, and μ is the factorization scale. The sum over k comprises the QCD penguin operators O_{3-6} and the electroweak penguin operators O_{7-10}. The C_i's are the Wilson coefficients which encode the short-distance physics. The four-quark operators O_i describing the hard electroweak process in b quark decays read

$$O_1^Q = \bar{Q}_\alpha \gamma_\mu (1 - \gamma_5) b_\beta \otimes \bar{s}_\beta \gamma^\mu (1 - \gamma_5) Q_\alpha,$$

$$O_2^Q = \bar{Q}_\alpha \gamma_\mu (1 - \gamma_5) b_\alpha \otimes \bar{s}_\beta \gamma^\mu (1 - \gamma_5) Q_\beta,$$

$$O_3 = \bar{s}_\beta \gamma_\mu (1 - \gamma_5) b_\beta \otimes \sum_{q'} \bar{q}'_\alpha \gamma^\mu (1 - \gamma_5) q'_\alpha,$$

$$O_4 = \bar{s}_\beta \gamma_\mu (1 - \gamma_5) b_\alpha \otimes \sum_{q'} \bar{q}'_\alpha \gamma^\mu (1 - \gamma_5) q'_\beta,$$

$$O_5 = \bar{s}_\beta \gamma_\mu (1 - \gamma_5) b_\beta \otimes \sum_{q'} \bar{q}'_\alpha \gamma^\mu (1 + \gamma_5) q'_\alpha,$$

$$O_6 = \bar{s}_\beta \gamma_\mu (1 - \gamma_5) b_\alpha \otimes \sum_{q'} \bar{q}'_\alpha \gamma^\mu (1 + \gamma_5) q'_\beta,$$

$$O_7 = \frac{3}{2} \bar{s}_\beta \gamma_\mu (1 - \gamma_5) b_\beta \otimes \sum_{q'} e_{q'} \bar{q}'_\alpha \gamma^\mu (1 + \gamma_5) q'_\alpha,$$

$$O_8 = \frac{3}{2} \bar{s}_\beta \gamma_\mu (1 - \gamma_5) b_\alpha \otimes \sum_{q'} e_{q'} \bar{q}'_\alpha \gamma^\mu (1 + \gamma_5) q'_\beta,$$

$$O_9 = \frac{3}{2} \bar{s}_\beta \gamma_\mu (1 - \gamma_5) b_\beta \otimes \sum_{q'} e_{q'} \bar{q}'_\alpha \gamma^\mu (1 - \gamma_5) q'_\alpha,$$

$$O_{10} = \frac{3}{2} \bar{s}_\beta \gamma_\mu (1 - \gamma_5) b_\alpha \otimes \sum_{q'} e_{q'} \bar{q}'_\alpha \gamma^\mu (1 - \gamma_5) q'_\beta, \quad (14)$$

where the sum over q' runs over the quark fields that are active at the scale $\mu = \mathcal{O}(m_b)$.

The decay amplitudes of $\Lambda_b \to \Lambda \eta_q$, $\Lambda_b \to \Lambda \eta_s$, and $\Lambda_b \to \Lambda \eta_c$ (namely, nonstrange $\mathcal{M}_q$, strange $\mathcal{M}_s$, and charm $\mathcal{M}_c$) are given by sandwiching $\mathcal{H}_{\text{eff}}$ with the initial and final states,

$$\mathcal{M}_{q,s,c} = \langle \Lambda \eta_{q,s,c} | \mathcal{H}_{\text{eff}} | \Lambda_b \rangle, \quad (15)$$

which can be further expanded with the Dirac spinors as

$$\mathcal{M} = \bar{\Lambda}(p')[M_S + M_P \gamma_5] \Lambda_b(p), \quad (16)$$

where M_S and M_P correspond to the parity-violating S-wave and parity-conserving P-wave amplitudes, respectively. Their generic factorization formula can be written as

$$M_{S/P} = \frac{f_{\Lambda_b} \pi^2 G_F}{18\sqrt{3}} \sum_{R_{ij}} \int [d^3x][d^3x'] dy [\mathcal{D}b]_{R_{ij}} \alpha_s^2(t_{R_{ij}})$$

$$\times \Omega_{R_{ij}}(b, b', b_q) e^{-S_{R_{ij}}} \sum_{\sigma=LL,LR,SP} a_{R_{ij}}^\sigma H_{R_{ij}}^\sigma(x, x', y),$$

$$(17)$$

where the summation extends over all possible diagrams R_{ij}. Here, $a_{R_{ij}}^\sigma$ denotes the product of the CKM matrix elements and the Wilson coefficients, where the superscripts $\sigma = LL$, LR, and SP refer to the contributions from $(V - A)(V - A)$, $(V - A)(V + A)$, and $(S - P)(S + P)$ operators, respectively. Notice that an overall factor 8 from

$a_{R_{ij}}^\sigma$ has been absorbed into the coefficient in Eq. (17) for convenience. The explicit forms of the Sudakov factors $S_{R_{ij}}$ can be found in [60]. Note that $H_{R_{ij}}^\sigma$ is the numerator of the hard amplitude depending on the spin structure of the final state, and $\Omega_{R_{ij}}$ is the Fourier transformation of the denominator of the hard amplitude from the k_T space to its conjugate b space. The impact parameters b, b', and b_q are conjugate to the parton transverse momenta k_T, k_T', and q_T, respectively. The integration measure of the momentum fractions is defined as

$$[d^3 x^{(')}] = dx_1^{(')} dx_2^{(')} dx_3^{(')} \delta(1 - x_1^{(')} - x_2^{(')} - x_3^{(')}), \quad (18)$$

where the δ functions enforce momentum conservation. The quantities associated with a specific diagram—such as $H_{R_{ij}}$, $a_{R_{ij}}$, $[\mathcal{D}b]_{R_{ij}}$, and $t_{R_{ij}}$—are collected in the Appendix. The decay branching ratios, up-down asymmetries, and direct CP asymmetries of the relevant decays are given as [73,75]

$$\mathcal{B} = \frac{|P|\tau_{\Lambda_b}}{8\pi} [(1 + r)^2 |M_S|^2 + (1 - r)^2 |M_P|^2],$$

$$\alpha = -\frac{2(1 - r^2) \text{Re}[M_S^* M_P]}{(1 + r)^2 |M_S|^2 + (1 - r)^2 |M_P|^2},$$

$$A_{CP} = \frac{\Gamma(\Lambda_b \to \Lambda \eta^{(')}) - \Gamma(\bar{\Lambda}_b \to \bar{\Lambda} \eta^{(')})}{\Gamma(\Lambda_b \to \Lambda \eta^{(')}) + \Gamma(\bar{\Lambda}_b \to \bar{\Lambda} \eta^{(')})}, \quad (19)$$

where $|P|$ is the magnitude of the three-momentum of the Λ baryon in the rest frame of the Λ_b baryon.

III. NUMERICAL ANALYSIS

In this section, we perform a numerical analysis for the branching ratios, up-down asymmetries, and direct CP asymmetries within various mixing schemes. As we have discussed before, there are four available mixing schemes for the $\eta - \eta'$ system, denoted as S1, S2, S3, and S4, respectively. We first collect the scheme dependent input parameters as follows:

(i) $\eta - \eta'$ mixing (S1) [3],

$$f_q = 1.07 f_\pi, \quad f_s = 1.34 f_\pi, \quad \phi = 39.3° \pm 1.0°,$$

$$m_0^q = 1.07 \text{ GeV}, \quad m_0^s = 1.92 \text{ GeV}. \quad (20)$$

(ii) $\eta - \eta' - G$ mixing (S2) [30],

$$f_q = f_\pi, \quad f_s = 1.3 f_\pi, \quad \phi = 43.7°,$$

$$\phi_G = 12° \pm 13°, \quad m_0^q = 2.08 \text{ GeV}, \quad m_0^s = 1.76 \text{ GeV}. \quad (21)$$

(iii) $\eta - \eta' - G - \eta_c$ mixing (S3) [6],

$$f_q = f_\pi, \quad f_s = 1.3 f_\pi, \quad \phi = 43.7°,$$
$$\phi_G = 12° \pm 13°, \quad m_0^q = 2.08 \text{ GeV}, \quad m_0^s = 1.76 \text{ GeV},$$
$$\phi_C = 11°, \quad f_{\eta_c} = 0.42 \text{ GeV}, \quad m_{\eta_c} = 2.98 \text{ GeV}. \quad (22)$$

(iv) $\eta - \eta' - \eta_c$ mixing (S4) [3],

$$f_q = 1.07 f_\pi, \quad f_s = 1.34 f_\pi, \quad \phi = 39.3° \pm 1.0°,$$
$$m_0^q = 1.79 \text{ GeV}, \qquad m_0^s = 1.91 \text{ GeV},$$
$$m_{\eta_c} = 2.95 \text{ GeV}, \qquad \theta_c = -1°,$$
$$\theta_y = -21.2°, \qquad f_{\eta_c} = 0.405 \text{ GeV}. \quad (23)$$

To obtain the chiral enhancement scales $m_0^{q,s}$, we also need the light quark mass as input. Because meson distribution amplitudes are defined at 1 GeV, we take $m_q(1 \text{ GeV}) = 5.6 \text{ MeV}$ [76] and $m_s(1 \text{ GeV}) = 0.13 \text{ GeV}$ [26]. The relevant masses (GeV) and the CKM parameters in Wolfenstein parametrization are taken from the Particle Data Group [18]. Their current values are

$$M = 5.6196, \qquad m_\Lambda = 1.116, \qquad m_b = 4.8,$$
$$m_c = 1.275, \qquad m_\eta = 0.548, \qquad m_{\eta'} = 0.958, \quad (24)$$

and

$$\lambda = 0.22650, \qquad A = 0.790,$$
$$\bar{\rho} = 0.141, \qquad \bar{\eta} = 0.357. \quad (25)$$

The lifetime of the Λ_b baryon is taken as 1.464 ps. For the pion decay constant, we use $f_\pi = 0.131 \text{ GeV}$ [64], and for the Gegenbauer moments, we choose $a_2 = 0.44 \pm 0.22$ and $a_4 = 0.25$ [28]. We neglect the scale dependence of the chiral scales and the Gegenbauer moments in the default calculation.

As stressed before, the PQCD calculations are performed in the quark-flavor basis. The contribution of various topological diagrams to a specific process is determined by the quark-flavor composition of the particles involved in the decay. For example, the nonstrange amplitude $\mathcal{M}_q$ receives contributions from all five topological diagrams, while the strange one $\mathcal{M}_s$ has no contributions from the C- and B-type diagrams. Note that the W exchange $bu \to su$ transition contributes to $\mathcal{M}_q$ and $\mathcal{M}_s$ through the E_q and E_s diagrams, respectively. As for the $\Lambda_b \to \Lambda\eta_c$ decay, besides the dominant T-type diagrams contributing to $\mathcal{M}_c$, it can proceed via B' diagrams if one replaces the $s\bar{s}$ pair with $c\bar{c}$ in the last diagram of Fig. 1.

According to Eq. (17), we first give the numerical results of various topology contributions to the S-wave and P-wave amplitudes for the $\Lambda_b \to \Lambda\eta_{q,s,c}$ processes within four mixing schemes in Table I. The differences among these solutions can be ascribed to the chiral enhancement scales related to the decay constants and the mixing angles. The drastic sensitivity of the chiral enhancement scales to

TABLE I. Numerical results of various topological amplitudes of $\Lambda_b \to \Lambda\eta_{q,s,c}$ in units of 10^{-10}. The last column is their sum. Only central values are presented here.

Scheme	T	C	E	B	B'	Total
$\Lambda_b \to \Lambda\eta_q$						
$M_S(\text{S1})$	$-3.8 + i1.2$	$3.2 - i15.3$	$-1.4 + i2.3$	$-2.4 + i3.1$	$0.7 - i0.3$	$-3.7 - i9.0$
$M_P(\text{S1})$	$-4.0 - i16.0$	$-3.3 + i12.5$	$-0.3 + i2.6$	$-1.8 - i6.8$	$-0.6 + i0.3$	$-10.0 - i7.4$
$M_S(\text{S2, S3})$	$-3.4 + i0.4$	$3.1 - i20.9$	$-1.4 + i3.3$	$-3.4 + i5.5$	$0.6 - i0.3$	$-4.5 - i12.0$
$M_P(\text{S2, S3})$	$-4.8 - i14.7$	$-2.6 + i17.1$	$-1.7 + i2.2$	$-5.1 - i7.6$	$-0.6 + i0.3$	$-14.8 - i2.7$
$M_S(\text{S4})$	$-3.8 + i1.2$	$4.4 - i20.9$	$-1.1 + i3.0$	$-3.6 + i4.3$	$0.7 - i0.3$	$-3.4 - i12.7$
$M_P(\text{S4})$	$-4.1 - i16.0$	$-2.4 + i16.7$	$-0.2 + i2.6$	$-4.7 - i7.1$	$-0.6 + i0.3$	$-12.0 - i3.5$
$\Lambda_b \to \Lambda\eta_s$						
$M_S(\text{S1})$	$-6.1 + i15.5$	$\cdots$	$4.0 - i8.5$	$\cdots$	$0.6 - i0.2$	$-1.5 + i6.8$
$M_P(\text{S1})$	$8.9 - i64.1$	$\cdots$	$-6.6 + i4.1$	$\cdots$	$-0.6 + i0.3$	$1.7 - i59.7$
$M_S(\text{S2, S3})$	$-4.1 + i9.5$	$\cdots$	$2.7 - i5.6$	$\cdots$	$0.4 - i0.2$	$-1.0 + i3.7$
$M_P(\text{S2, S3})$	$6.6 - i43.2$	$\cdots$	$-4.5 + i2.1$	$\cdots$	$-0.4 + i0.2$	$1.7 - i40.9$
$M_S(\text{S4})$	$-5.8 + i14.8$	$\cdots$	$4.0 - i8.5$	$\cdots$	$0.6 - i0.2$	$-1.2 + i6.1$
$M_P(\text{S4})$	$10.5 - i63.8$	$\cdots$	$-6.0 + i4.9$	$\cdots$	$-0.6 + i0.3$	$3.9 - i58.6$
$\Lambda_b \to \Lambda\eta_c$						
$M_S(\text{S3})$	$42.8 - i369.9$	$\cdots$	$\cdots$	$\cdots$	$0.05 + i0.02$	$42.9 - i369.9$
$M_P(\text{S3})$	$80.9 - i583.9$	$\cdots$	$\cdots$	$\cdots$	$-0.05 + i0.01$	$80.8 - i583.9$
$M_S(\text{S4})$	$35.4 - i356.0$	$\cdots$	$\cdots$	$\cdots$	$0.04 + i0.01$	$35.4 - i356.0$
$M_P(\text{S4})$	$74.3 - i576.9$	$\cdots$	$\cdots$	$\cdots$	$-0.05 + i0.01$	$74.3 - i576.9$

the choice of mixing schemes will be reflected in the spread of our predictions for the decay amplitudes. Referring to Eqs. (20) and (21), we can see that the chiral scale m_0^q in S2 is almost twice as large as that in S1, causing distinct nonstrange amplitudes for the two schemes. Analogously, the m_0^s in S1 and S4 are almost equal, resulting in a tiny variation in the strange amplitudes. Likewise, the same mixing parameters are used in S2 and S3 as shown in Eqs. (21) and (22); the calculated amplitudes are exactly the same. Numerical differences between S3 and S4 for the charm amplitude arise from a different choice of mass and decay constants of the η_c meson as shown in Eqs. (22) and (23). One may wonder why the T-type nonstrange amplitudes yield the same results under S1 and S4 despite the fact that the parameter m_0^q differs between the two schemes. The interpretation is not trivial. We know that the chiral scales are proportional to the twist-3 meson LCDAs, which do not contribute to the nonstrange amplitude via the external W emission diagram at the current theoretical accuracy (see the expression of $H_{T_{c7}}^\sigma$ in Table VII, for example) because only the external W emission from $(V-A)(V-A)$ and $(S-P)(S+P)$ operators survives for the $b \to su\bar{u}$ and $b \to sd\bar{d}$ transitions. Nevertheless, the strange amplitude receives additional twist-3 contributions arising from the W emission diagrams through the $b \to ss\bar{s}$ transition with the $(V-A)(V+A)$ operators inserted. As a result, the m_0^s term appears in the strange amplitude, resulting in the different T-type strange amplitudes between S1 and S4.

We now proceed to discuss the relative sizes of various topological amplitudes. From Table I, we observe that the $\Lambda_b \to \Lambda\eta_q$ process is dominated by T and C. As the interference between T and C is destructive, the contributions from the exchange diagrams, such as B and E, are in fact important and non-negligible. Similar to the case of $\Lambda_b \to \Lambda\phi$ [60], the $\Lambda_b \to \Lambda\eta_s$ decay is governed by T and

E, which are of similar sizes. The $\Lambda_b \to \Lambda\eta_c$ process is dominated by the T-type diagrams, and its amplitudes are larger than the (non)strange ones by 1 order of magnitude. The contributions from B'-type exchange diagrams are predicted to be negligibly small in all three processes.

It is worth noting that the penguin operators could be inserted into the diagrams in Fig. 1 via the Fierz transformation. We do not distinguish between the tree and penguin contributions in Table I. The tree contributions of the strange and nonstrange amplitudes are expected to be small due to the CKM suppressed compared to the penguin ones. If we turn off the penguin contributions, their total amplitudes will decrease by 1 or 2 orders of magnitude. This feature is different for the charm one, which is triggered by the quark decay $b \to sc\bar{c}$. The large CKM matrix element $V_{cb}V_{cs}^*$ enhances the tree contributions, which dominate over the penguin ones.

Utilizing the values of Table I in conjunction with various mixing formalisms, one can calculate the S- and P-wave amplitudes of $\Lambda_b \to \Lambda\eta^{(\prime)}$, whose numerical results are displayed in Table II. Branching ratios, up-down asymmetries, and the direct CP asymmetries are shown in the last three columns. There are four uncertainties. The first quoted uncertainty is due to the shape parameters ω_0 in the Λ_b LCDAs with 10% variation. The second uncertainty is caused by the variation of the Gegenbauer moment $a_2 = 0.44 \pm 0.22$ in the leading-twist LCDAs of $\eta_{q,s}$. Since the Gegenbauer moment a_2 is not yet well determined, the possible 50% variation leads to large changes of our predictions. The third one refers to the uncertainty of the mixing angles $\phi(\phi_G)$ as shown in Eqs. (20)–(23). Note that the chiral enhancement scale m_0^q changes rapidly with the mixing angles, so this uncertainty can be classified as the hadronic parameter uncertainty. The last one is from the hard scale t varying from $0.8t$ to $1.2t$. The scale-dependent uncertainty can be reduced only if the

TABLE II. Magnitudes of the S- and P-wave amplitudes (in units of 10^{-10}), branching ratios (in units of 10^{-6}), up-down asymmetries, and direct CP violations of $\Lambda_b \to \Lambda\eta^{(\prime)}$ decays with different mixing schemes. The errors for these entries correspond to the shape parameter ω_0, Gegenbauer moment a_2, mixing angles $\phi(\phi_G)$, and the hard scale t, respectively.

Scheme	M_S	M_P	$\mathcal{B}(10^{-6})$	α	$A_{CP}(\%)$
$\Lambda_b \to \Lambda\eta$					
S1	$-1.9 - i11.2$	$-8.9 + i32.1$	$2.13^{+0.35+0.01+0.46+1.03}_{-0.41-0.01-0.26-0.60}$	$0.734^{+0.087+0.102+0.000+0.004}_{-0.041-0.266-0.090-0.097}$	$1.9^{+0.2+1.8+4.0+3.3}_{-2.5-4.8-0.0-0.0}$
S2	$-2.5 - i11.2$	$-11.8 + i26.4$	$1.73^{+0.39+0.00+0.15+0.41}_{-0.54-0.19-0.68-0.42}$	$0.702^{+0.012+0.182+0.000+0.091}_{-0.018-0.088-0.074-0.041}$	$8.8^{+0.0+0.0+0.0+3.2}_{-6.7-9.7-7.7-6.9}$
S3	$-2.2 - i14.0$	$-11.2 + i22.0$	$1.61^{+0.35+0.00+0.27+0.42}_{-0.52-0.18-0.70-0.41}$	$0.800^{+0.039+0.119+0.028+0.064}_{-0.000-0.028-0.130-0.013}$	$8.1^{+0.0+0.0+0.0+3.0}_{-8.6-7.0-2.9-5.7}$
S4	$-2.1 - i11.5$	$-12.2 + i37.7$	$2.86^{+1.02+0.05+0.83+1.34}_{-0.64-0.24-0.53-0.81}$	$0.650^{+0.000+0.047+0.032+0.025}_{-0.073-0.267-0.130-0.027}$	$5.7^{+0.0+0.0+0.0+0.0}_{-1.5-7.8-3.5-4.0}$
$\Lambda_b \to \Lambda\eta'$					
S1	$-3.5 - i0.5$	$-5.0 - i50.9$	$3.94^{+0.92+1.20+0.00+1.21}_{-0.65-0.94-0.30-1.14}$	$-0.046^{+0.127+0.344+0.154+0.098}_{-0.148-0.261-0.094-0.000}$	$5.5^{+0.0+1.4+0.0+0.0}_{-3.4-2.8-4.5-6.6}$
S2	$-3.7 - i5.4$	$-8.7 - i30.9$	$1.68^{+0.25+0.50+0.00+0.49}_{-0.55-0.55-0.15-0.53}$	$-0.531^{+0.247+0.226+0.354+0.030}_{-0.154-0.173-0.173-0.014}$	$3.7^{+0.0+1.1+2.0+3.7}_{-9.8-5.4-2.4-0.1}$
S3	$-2.1 - i19.8$	$-5.6 - i53.6$	$5.67^{+1.34+1.19+6.48+1.37}_{-1.65-1.22-4.20-1.25}$	$-0.847^{+0.068+0.042+0.180+0.002}_{-0.055-0.047-0.030-0.007}$	$0.3^{+0.0+1.0+6.2+3.0}_{-5.5-0.6-2.7-0.4}$
S4	$-3.6 + i2.3$	$-5.7 - i38.1$	$2.28^{+0.46+0.84+0.52+0.93}_{-0.25-0.18-0.00-0.36}$	$0.134^{+0.193+0.490+0.278+0.154}_{-0.193-0.249-0.260-0.006}$	$-0.4^{+5.6+8.7+9.2+11.2}_{-0.0-0.0-0.0-0.0}$

next-to-leading order contributions in the PQCD approach are included. One can see that these large hadronic parameter uncertainties have a crucial influence on the PQCD calculations. The up-down asymmetries from large theoretical errors, especially for the values in S4, due to complex interference effects, which will be detailed later. It is interesting that $\mathcal{B}(\Lambda_b \to \Lambda\eta')$ in S3 is more sensitive to ϕ_G. The phenomena could be ascribed to the sizable η_c mixing effect in S3. According to Eq. (4), the charm amplitude for the η' mode suffers from the suppression from the mixing factor $\cos\theta \sin\phi_G \sin\phi_C = 0.039^{+0.040}_{-0.042}$, where the large uncertainty is due to the angle ϕ_G, which varies in a conservative range $\phi_G = 12° \pm 13°$. Moreover, the large $\Lambda_b \to \Lambda\eta_c$ amplitude, as indicated in Table I, can compensate for this suppression and give a sizable impact on the $\Lambda_b \to \Lambda\eta'$ decay. For the η mode, the corresponding mixing factor is $-\sin\theta \sin\phi_G \sin\phi_C = -0.0076^{+0.0078}_{-0.0082}$, which is smaller by a factor of 5. It follows that it does not have much impact on the decay rates involving η.

We now discuss the sensitivity of the branching ratios of the $\Lambda_b \to \Lambda\eta^{(')}$ to different mixing schemes. From Table II, one can see clearly that the results of the η mode are less sensitive to the mixing schemes, which suggests small gluonic and η_c components in the η meson. The marginal differences among various schemes can be more or less traced to the different chiral enhancement scales as already emphasized. However, various schemes lead to very different branching ratios for the η' channel. For example, the central values vary from 1.68×10^{-6} for S2 to 5.67×10^{-6} for S3. The biggest branching ratio from S3 is ascribed to the fact that in the $\eta - \eta' - G - \eta_c$ mixing scheme, the tree dominated $\Lambda_b \to \Lambda\eta_c$ amplitude, induced from the $b \to sc\bar{c}$ transition, can contribute to the $\Lambda_b \to \Lambda\eta^{(')}$ decays through the mixing matrix as indicated in Eq. (4). As stated above, the large charm amplitude can compensate for the tiny mixing factor, which implies that the component of η_c in the η' meson is important. Our results indicate that the obtained branching ratios for $\Lambda_b \to \Lambda\eta$ and $\Lambda_b \to \Lambda\eta'$ are comparable in magnitude. This observation is different from the pattern of $\mathcal{B}(B \to K\eta)$ and $\mathcal{B}(B \to K\eta')$, where the former is about an order of magnitude smaller than the latter.

In Ref. [77], the authors point out that few-percent OZI violating effects, neglected in the FKS scheme, could enhance the chiral scale m_0^q sufficiently, which accommodates the dramatically different data of the $B \to K\eta^{(')}$ branching ratios in the PQCD approach. It is therefore interesting to see whether this effect can modify the pattern of $\Lambda_b \to \Lambda\eta^{(')}$ branching ratios and improve the agreement with the current data. It should be noted that the inclusion of the OZI violating effects implies two additional twist-2 meson distribution amplitudes associated with the OZI violating decay constants that need to be considered, but their contributions turn out to be insignificant [77]. Hence,

we can simply concentrate on the effect of the modified parameter set. Using the central values of $f_q = 1.10 f_\pi$, $f_s = 1.46 f_\pi$, $\phi = 36.84°$, $m_0^q = 4.32$ GeV, $m_0^s = 1.94$ GeV from [77] as inputs, we derive

$$\mathcal{B}(\Lambda_b \to \Lambda\eta) = 5.45 \times 10^{-6},$$
$$\mathcal{B}(\Lambda_b \to \Lambda\eta') = 3.91 \times 10^{-6}. \qquad (26)$$

We will see later that by including the OZI violating effects in S1, $\mathcal{B}(\Lambda_b \to \Lambda\eta)$ tend to be large, while $\mathcal{B}(\Lambda_b \to \Lambda\eta')$ tend to be small, as favored by the experiments.

For the up-down asymmetries of the η mode, all four solutions basically exhibit a similar pattern in size and sign. However, the observation is different for the η' channel: From Table II we see that S2 and S3 give large and negative asymmetries, while the central values in S1 and S4 are small in magnitude but with opposite signs. These features can be understood by the following observation. We learn that α describes the interference between the S-wave and P-wave amplitudes from Eq. (19). According to the mixing matrices described in the previous section, both the S-wave and P-wave amplitudes in $\Lambda_b \to \Lambda\eta^{(')}$ decays can be written as the linear superposition of strange and non-strange amplitudes through the mixing angle. It should be noted that the nonstrange contents of the η and η' mesons have the same sign in S1, while the strange ones are opposite in sign. This means the interference between the strange and nonstrange amplitudes is always destructive in $\Lambda_b \to \Lambda\eta$ but constructive in $\Lambda_b \to \Lambda\eta'$. In addition, compared to the strange amplitude, the nonstrange amplitude acquires additional sizable contributions from the internal W emission diagrams as shown in Fig. 1, which leads to different patterns of the S-wave and P-wave contributions in the strange and nonstrange amplitudes. Numerically, one can see from Table II that the P-wave component dominates over the S-wave one in the η' mode, whereas they are comparable in the η one. The above combined effects cause the imaginary parts of the S-wave amplitudes of $\Lambda_b \to \Lambda\eta$ and $\Lambda_b \to \Lambda\eta'$ to have the same sign, while the P-wave ones have the opposite sign as exhibited in Table II. Consequently, the up-down asymmetries of $\Lambda_b \to \Lambda\eta$ and $\Lambda_b \to \Lambda\eta'$ are of opposite sign. The feature in the S2 scheme can be explained in a similar way. The interference pattern is more complicated with the inclusion of the charm content in the $\eta^{(')}$ mesons within S3 and S4. We have learned from Eqs. (4) and (2) that the charm contents of the $\eta^{(')}$ meson for the two mixing schemes are opposite (same) in sign. This difference has very little effect on the η mode because of the strong suppression from the mixing factors; however, it has an important influence on the η' one as discussed before. We predict a large and negative $\alpha(\Lambda_b \to \Lambda\eta')$ in S3 but a small and positive one in S4.

TABLE III.   Various predictions in the literature of the $\Lambda_b \to \Lambda\eta^{(')}$ decays. Experimental measurements are taken from Ref. [34].

	LFQM [35]	QCDF [36]	GFA [37]	GFA [78]	QCDSR [38]	PM [38]	LHCb [34]
$\mathcal{B}(\Lambda_b \to \Lambda\eta)$	5.46×10^{-8}	4.39×10^{-7}	$(1.47 \pm 0.35) \times 10^{-6}$	$(1.59^{+0.45}_{-0.29}) \times 10^{-6}$	11.47×10^{-6}	2.95×10^{-6}	$9.3^{+7.3}_{-5.3} \times 10^{-6}$
$\mathcal{B}(\Lambda_b \to \Lambda\eta')$	2.29×10^{-8}	4.03×10^{-6}	$(1.83 \pm 0.58) \times 10^{-6}$	$(1.90^{+0.74}_{-0.36}) \times 10^{-6}$	11.33×10^{-6}	3.24×10^{-6}	$< 3.1 \times 10^{-6}$
$\alpha(\Lambda_b \to \Lambda\eta)$	-1	$0.24^{+0.19}_{-0.12}$	$\cdots$	$\cdots$	$\cdots$	$\cdots$	$\cdots$
$\alpha(\Lambda_b \to \Lambda\eta')$	-1	$0.99^{+0.00}_{-0.03}$	$\cdots$	$\cdots$	$\cdots$	$\cdots$	$\cdots$
$A_{CP}(\Lambda_b \to \Lambda\eta)$	$\cdots$	$(-3.4^{+0.6}_{-0.4})\%$	$\cdots$	$(0.4 \pm 0.2)\%$	$\cdots$	$\cdots$	$\cdots$
$A_{CP}(\Lambda_b \to \Lambda\eta')$	$\cdots$	$(1.0^{+0.1}_{-0.2})\%$	$\cdots$	$(1.6 \pm 0.1)\%$	$\cdots$	$\cdots$	$\cdots$

Since the decays under consideration are dominated by the penguin contribution and the tree amplitudes are color and CKM factor suppressed, their direct CP asymmetries are not large, less than 10%. Although the additional tree amplitudes stemming from the $b \to sc\bar{c}$ transition are included in S3 and S4, the weak phase of $V_{cb}V_{cs}^*$ is zero at the order of λ^2, which is the same as the penguin one, $V_{tb}V_{ts}^*$. The enhancement arising from the charm content in fact leads to a smaller tree-over-penguin ratio, and thus the direct CP asymmetries of the η' process in S3 and S4 are further reduced to less than one percent.

The comparisons with different theoretical models and the experimental data are presented in Table III. There is a wide spread in the branching ratios predicted by the various model calculations, ranging from 10^{-8} to 10^{-5}. The LFQM calculations [35] give the lowest predictions for the branching ratios because only the contributions from the tree operators were considered in their calculations, which implies the penguin contributions play leading roles in the relevant processes. In the absence of the penguin contributions, our central values of the branching ratios for the η and η' modes in S1 will be reduced to 8.92×10^{-8} and 4.14×10^{-8}, respectively, which seem to be comparable to the results of LFQM [35]. The two solutions of Ref. [38] are evaluated by using two different $\Lambda_b \to \Lambda$ form factors. The branching ratios for the form factors calculated in the pole model (PM) agree with our PQCD predictions within the S1 and S4 mixing schemes. The two results from GFA [37,78] are basically consistent with each other and close to our values in S2. It is also observed in Table III that most of the approaches give predictions of the same order of magnitude for the decay rates of the two modes, except for the predictions of Ref. [36], in which the branching ratio for the η' mode is much larger than that of η by 1 order of magnitude due to the additional enhanced factor for the η' mode.

It should be noted that the previous theoretical calculations are based on the S1 scheme and do not take into account the contributions from the exchange amplitudes. As seen in Table I, the emission amplitudes generally dominate over the exchange ones in PQCD calculations, so we can drop all the exchange amplitudes and focus on the S1 mixing scenario to obtain a simple picture

for the relevant decays. The resulting central values of the branching ratios are $\mathcal{B}(\Lambda_b \to \Lambda\eta) = 3.89 \times 10^{-6}$ and $\mathcal{B}(\Lambda_b \to \Lambda\eta') = 4.13 \times 10^{-6}$, indicating that our predictions in Table I can be roughly reproduced under this simple picture. This implies other processes governed by the T and C topologies have the branching ratios of 10^{-6} as well. For the charmless decays $\Lambda_b \to \Lambda M$, there are six more processes with $M = \pi, \rho, K, K^*, \phi, \omega$, which are dominated by the emission diagrams. The ρ and π modes belong to the isospin-violating decays; thus, they have no QCD penguin contributions. The K and K^* modes are induced by the $b \to d$ transitions, which are CKM suppressed. As such, the four processes should have substantially lower rates than 10^{-6}. The ϕ mode is studied in PQCD [60], and its branching ratio is predicted to be of the order 10^{-6}, which is comparable to the data. There is currently no PQCD prediction or experimental data for the ω mode. Because the ω meson has the same quark content as the η_q meson, we estimate its branching ratio in PQCD to be 10^{-6}. This estimation is likely to be beneficial in experimental searches for these modes.

Unlike the branching ratios, up-down asymmetries, and CP asymmetries in the relevant decays have received little attention in theoretical and experimental studies. The estimates based on QCDF give $\alpha(\Lambda_b \to \Lambda\eta) = 0.24^{+0.19}_{-0.12}$ and $\alpha(\Lambda_b \to \Lambda\eta') = 0.99^{+0.00}_{-0.03}$ [36], while the LFQM calculations yield $\alpha(\Lambda_b \to \Lambda\eta) = \alpha(\Lambda_b \to \Lambda\eta') = -1$ [35]. It can be observed that the available theoretical predictions on the up-down asymmetries vary and differ even in sign. Hence, an accurate measurement of the up-down asymmetry will enable us to discern different models. For the direct CP violation, nearly all of the current theoretical predictions are small, less than 10% in magnitude.

From the experimental data shown in Table III, it is clear that LHCb's measurement of $\mathcal{B}(\Lambda_b \to \Lambda\eta)$ [34] is generally larger than the theoretical expectations. Although the prediction of Ref. [38] is in accordance with the central value of the data, its value of $\mathcal{B}(\Lambda_b \to \Lambda\eta')$ exceeds the present experimental bound by a factor of 3. The PQCD results of $\mathcal{B}(\Lambda_b \to \Lambda\eta')$ based on the S1 and S3 mixing schemes are also large compared to the experimental upper limit. In particular, the latter is larger by a factor of 2, which indicates the mixing angles ϕ_G and/or ϕ_C may be

overestimated. Of course, the measurement was performed in 2015, and the experimental error was also quite large. Moreover, there are still no available data on the up-down and direct CP asymmetries at the moment. We look forward to more experimental efforts to improve the accuracy of the relevant measurements.

As a by-product, we have predicted the decay branching ratio and up-down asymmetry of the $\Lambda_b \to \Lambda\eta_c$ mode by using the values of the charm amplitudes in Table I. Explicitly, we obtain

$$\mathcal{B}(\Lambda_b \to \Lambda\eta_c) = \begin{cases} (6.83^{+2.10+1.37}_{-0.99-0.24}) \times 10^{-4} & \text{for S3} \\ (6.55^{+1.73+0.91}_{-1.32-0.59}) \times 10^{-4} & \text{for S4} \end{cases} \quad (27)$$

and

$$\alpha(\Lambda_b \to \Lambda\eta_c) = \begin{cases} -0.998^{+0.002+0.001}_{-0.000-0.000} & \text{for S3} \\ -0.996^{+0.000+0.001}_{-0.000-0.001} & \text{for S4}, \end{cases} \quad (28)$$

where the first and second sets of error bars are due to the shape parameter $\omega_0 = 0.40 \pm 0.04$ GeV in the Λ_b baryon LCDAs and the hard scale t varying from $0.8t$ to $1.2t$, respectively. Our branching ratio is much larger than the values of $(2.47^{+0.33+0.42+0.67}_{-0.19-0.47-0.23}) \times 10^{-4}$ in QCDF [36] and $(1.5 \pm 0.9) \times 10^{-4}$ in GFA [79]. This is not surprising because the PQCD prediction on the branching ratio of the J/ψ mode presented in [59] is also generally larger than the corresponding values from [36,79] due to the significant nonfactorizable contributions. All of these theoretical predictions are at the order of 10^{-4}, which can be accessible to the experiments at the LHCb. The predicted up-down asymmetry is nearly 100% and negative, which is consistent with the value of -0.99 ± 0.00 obtained in [36]. Since both the tree and penguin amplitudes have no weak phase to order λ^2, the direct CP violation for the $\Lambda_b \to \Lambda\eta_c$ process is predicted to be zero.

IV. CONCLUSION

Decays of b hadrons to two-body final states containing an η or η' meson are of great phenomenological importance. These processes could provide useful information about the $\eta - \eta'$ mixing and the structure of the η and η' mesons, which is still a long-standing question in the literature. In this work, we have carried out a systematic study of the penguin-dominant $\Lambda_b \to \Lambda\eta^{(')}$ decays in the PQCD approach. The calculations are performed in the quark-flavor mixing basis, in which we first give the PQCD predictions on the nonstrange, strange, and charm amplitudes including various topological contributions. It is observed that the nonstrange amplitude is dominated by the T- and C-type diagrams. As the interference between T and C is destructive, the contributions from the exchange diagrams, such as B and E, are in fact important and

non-negligible. The strange amplitude is governed by T and E, which are of similar sizes. The charm one is dominated by the T-type diagrams, and its amplitudes are larger than the (non)strange ones by 1 order of magnitude. Furthermore, the contributions from B'-type exchange diagrams are predicted to be negligibly small for all three amplitudes.

Utilizing the four available mixing schemes for the $\eta - \eta'$ system—namely, $\eta - \eta'$, $\eta - \eta' - G$, $\eta - \eta' - G - \eta_c$, and $\eta - \eta' - \eta_c$ mixing, denoted, respectively, as S1, S2, S3, and S4—we evaluate the branching ratios, up-down asymmetries, and direct CP asymmetries for $\Lambda_b \to \Lambda\eta^{(')}$ decays and investigate the scheme dependence of our theoretical predictions. We find that the results of the η mode are less sensitive to the mixing schemes, which implies small gluonic and η_c components in the η meson. However, various schemes lead to quite different predictions on both the branching ratio and up-down asymmetry for the channel involving η'. For instance, $\mathcal{B}(\Lambda_b \to \Lambda\eta')$ increases by a factor of 3 from S2 to S3, while $\alpha(\Lambda_b \to \Lambda\eta')$ varies from -0.046 for S1 to -0.847 for S3 and even flips signs in S4. The large discrepancy among these solutions suggests the η' mode is very useful in discriminating various mixing schemes.

We consider theoretical uncertainties arising from the shape parameter ω_0, Gegenbauer moment a_2, mixing angles $\phi(\phi_G)$, and the hard scale t. We show the nontrivial dependence of the PQCD calculations on the nonperturbative hadronic parameters, which are poorly determined at present. In particular, $\mathcal{B}(\Lambda_b \to \Lambda\eta')$ is extremely sensitive to the variation of ϕ_G and thus a good candidate for constraining the mixing parameters, once it is measured with sufficient accuracy. The scale-dependent uncertainty also gives large uncertainties to the branching ratios, which can be reduced only if the next-to-leading order contributions in the PQCD approach are known.

We also compare our results with predictions of the other theoretical approaches as well as existing experimental data. Various model estimations on the branching ratios span fairly wide ranges from 10^{-8} to 10^{-5}. Our branching ratios for the S2 scheme are consistent with the GFA calculations, while the S4 ones are close to the results of the PM. The predicted central values of $\mathcal{B}(\Lambda_b \to \Lambda\eta)$ in various schemes are generally lower than the measurement from LHCb. The inclusion of OZI violating effects can enhance $\mathcal{B}(\Lambda_b \to \Lambda\eta)$ by a factor of 2.5 and improve the agreement with the current data. The PQCD results of $\mathcal{B}(\Lambda_b \to \Lambda\eta')$ based on S1 and S3 mixing schemes exceed the present experimental bound. Note that the measured branching ratios also have large uncertainties. In general, the values in S4 appear to be more preferred by the current data among these solutions. For the up-down asymmetries, there are considerable deviations among PQCD, QCDF, and LFQM estimates, which should be clarified in the future. On the other hand, since the tree contributions suffer from the color suppression and CKM suppression, the obtained direct CP

asymmetries are less than 10%, in comparison with the numbers from QCDF and GFA. At the moment, there is neither experimental information on the up-down asymmetries nor on direct CP asymmetries. It will be interesting to see the updated measurements on the two decay modes.

Finally, we explore the decay of $\Lambda_b \to \Lambda\eta_c$. The estimated branching ratio is at the 10^{-4} level with an up-down asymmetry close to -1, which may shed light on future measurements.

ACKNOWLEDGMENTS

APPENDIX: FACTORIZATION FORMULAS

Following the conventions in Ref. [73], we provide some details about the factorization formulas in Eq. (17) for the nonstrange amplitude, which were not given before. As the strange and charm processes have the same decay topologies as $\Lambda_b \to \Lambda\phi$ and $\Lambda_b \to \Lambda J/\psi$ modes, respectively, one can find the relevant formulas in our previous work [59,60]. The combinations of the Wilson coefficients $a^\sigma_{R_{ij}}$ and the b dependent quantities $[\mathcal{D}b]_{R_{ij}}$ and $\Omega_{R_{ij}}$ are given in Tables IV and V, respectively, and the auxiliary functions $h_{1,2,3}$ and the Bessel function K_0 can be found in [73].

The hard scale t for each diagram is chosen as the maximal virtuality of internal particles including the factorization scales in a hard amplitude:

$$t_{R_{ij}} = \max\left(\sqrt{|t_A|}, \sqrt{|t_B|}, \sqrt{|t_C|}, \sqrt{|t_D|}, w, w', w_q\right), \quad \text{(A1)}$$

where the expressions of $t_{A,B,C,D}$ are listed in Table VI. The factorization scales w, w', and w_q are defined by

$$w^{(')} = \min\left(\frac{1}{b_1^{(')}}, \frac{1}{b_2^{(')}}, \frac{1}{b_3^{(')}}\right), \qquad w_q = \frac{1}{b_q}, \quad \text{(A2)}$$

with the variables

TABLE IV. Expressions of a^{LL} and a^{SP} in the $\Lambda_b \to \Lambda\eta_q$ decay. For convenience, we have extracted an overall coefficient 8, which is absorbed into the prefactor in Eq. (17).

R_{ij}	a^{LL}	a^{SP}
$T_{a1,a2,a3,a5,b1,b2,b4}$	$\frac{1}{3}V_{ub}V_{us}^*[C_1 + \frac{1}{3}C_2] - \frac{1}{3}V_{tb}V_{ts}^*[2C_3 + \frac{2}{3}C_4 + \frac{1}{2}C_9 + \frac{1}{6}C_{10}]$	$-\frac{1}{3}V_{tb}V_{ts}^*[2C_5 + \frac{2}{3}C_6 + \frac{1}{2}C_7 + \frac{1}{6}C_8]$
$T_{a6,a7,b6,b7,c1,c2,d1,d2}$	$\frac{1}{3}V_{ub}V_{us}^*C_2 - \frac{1}{3}V_{tb}V_{ts}^*[2C_4 + \frac{1}{2}C_{10}]$	$-\frac{1}{3}V_{tb}V_{ts}^*[2C_6 + \frac{1}{2}C_8]$
$T_{c5,c7,d6}$	$V_{ub}V_{us}^*[-\frac{1}{4}C_1 + \frac{1}{3}C_2] + V_{tb}V_{ts}^*[\frac{1}{2}C_3 - \frac{2}{3}C_4 + \frac{1}{8}C_9 - \frac{1}{6}C_{10}]$	$V_{tb}V_{ts}^*[\frac{1}{2}C_5 - \frac{2}{3}C_6 + \frac{1}{8}C_7 - \frac{1}{6}C_8]$
$C_{a1-a4,b1,b3,c1,c3,d1-d3,e1,f1}$		
$Eq_{a1-a7,e1-e4,f2}$	$\frac{1}{3}V_{ub}V_{us}^*[C_1 - C_2] - \frac{1}{6}V_{tb}V_{ts}^*[4C_3 - 4C_4 + C_9 - C_{10}]$	$-\frac{1}{6}V_{tb}V_{ts}^*[4C_5 - 4C_6 + C_7 - C_8]$
$B_{a1-a4,b1,b3,c1,c4,d1,d2,d4,d5}$		
$C_{a5,b4,c4,e2},\ Eq_{b1,b3,b4,b7}$	$-\frac{1}{3}V_{ub}V_{us}^*[2C_1 + C_2] + \frac{1}{3}V_{tb}V_{ts}^*[4C_3 + 2C_4 + C_9 + \frac{1}{2}C_{10}]$	$\frac{1}{3}V_{tb}V_{ts}^*[4C_5 + 2C_6 + C_7 + \frac{1}{2}C_8]$
$C_{a6,b6,c5,e3},\ Eq_{c1,c2,c3,c7}$	$\frac{1}{3}V_{ub}V_{us}^*[C_1 - 2C_2] - \frac{1}{3}V_{tb}V_{ts}^*[2C_3 + 4C_4 + \frac{1}{2}C_9 + C_{10}]$	$-\frac{1}{3}V_{tb}V_{ts}^*[2C_5 + 4C_6 + \frac{1}{2}C_7 + C_8]$
$C_{a7,b7,c7,d7,e4},\ Eq_{d1-d4,d7}$	$\frac{1}{3}V_{ub}V_{us}^*[-2C_1 + 2C_2] + \frac{1}{3}V_{tb}V_{ts}^*[4C_3 - 4C_4 + C_9 - C_{10}]$	$\frac{1}{3}V_{tb}V_{ts}^*[4C_5 - 4C_6 + C_7 - C_8]$
$B_{a7,b7,c7,d7,e1-e4}$		
$C_{b2},\ Eq_{f1},\ B_{b2,c5}$	$\frac{1}{3}V_{ub}V_{us}^*[-\frac{5}{4}C_1 - C_2] + V_{tb}V_{ts}^*[\frac{5}{6}C_3 + \frac{2}{3}C_4 + \frac{5}{24}C_9 + \frac{1}{6}C_{10}]$	$V_{tb}V_{ts}^*[\frac{5}{6}C_5 + \frac{2}{3}C_6 + \frac{5}{24}C_7 + \frac{1}{6}C_8]$
$C_{b5,d4,f2},\ Eq_{b2,b5,b6},\ B_{d1}$	$\frac{1}{3}V_{ub}V_{us}^*[\frac{1}{4}C_1 - C_2] - V_{tb}V_{ts}^*[\frac{1}{6}C_3 - \frac{2}{3}C_4 + \frac{1}{24}C_9 - \frac{1}{6}C_{10}]$	$-V_{tb}V_{ts}^*[\frac{1}{6}C_5 - \frac{2}{3}C_6 + \frac{1}{24}C_7 - \frac{1}{6}C_8]$
$C_{c2},\ Eq_{f3},\ B_{b5,c3}$	$\frac{1}{3}V_{ub}V_{us}^*[C_1 + \frac{5}{4}C_2] - V_{tb}V_{ts}^*[\frac{2}{3}C_3 + \frac{5}{6}C_4 + \frac{1}{6}C_9 + \frac{5}{24}C_{10}]$	$-V_{tb}V_{ts}^*[\frac{2}{3}C_5 + \frac{5}{6}C_6 + \frac{1}{6}C_7 + \frac{5}{24}C_8]$
$C_{c6,f3},\ Eq_{c4,c5,c6}$	$\frac{1}{3}V_{ub}V_{us}^*[C_1 - \frac{1}{4}C_2] - V_{tb}V_{ts}^*[\frac{2}{3}C_3 - \frac{1}{6}C_4 + \frac{1}{6}C_9 - \frac{1}{24}C_{10}]$	$-V_{tb}V_{ts}^*[\frac{2}{3}C_5 - \frac{1}{6}C_6 + \frac{1}{6}C_7 - \frac{1}{24}C_8]$
$C_{d5,d6,f4},\ Eq_{d5,d6},\ B_{a6,c6,d6,f1-f4}$	$\frac{1}{12}V_{ub}V_{us}^*[C_1 - C_2] - V_{tb}V_{ts}^*[\frac{1}{6}C_3 - \frac{1}{6}C_4 + \frac{1}{24}C_9 - \frac{1}{24}C_{10}]$	$-V_{tb}V_{ts}^*[\frac{1}{6}C_5 - \frac{1}{6}C_6 + \frac{1}{24}C_7 - \frac{1}{24}C_8]$
$Eq_{f4},\ B_{a5,b4,c2,d3}$	$-\frac{5}{12}V_{ub}V_{us}^*[C_1 - C_2] + V_{tb}V_{ts}^*[\frac{5}{6}C_3 - \frac{5}{6}C_4 + \frac{5}{24}C_9 - \frac{5}{24}C_{10}]$	$V_{tb}V_{ts}^*[\frac{5}{6}C_5 - \frac{5}{6}C_6 + \frac{5}{24}C_7 - \frac{5}{24}C_8]$
$C_{g1},\ Eq_{g2}$	0	0
C_{g2}	$-\frac{3}{4}V_{ub}V_{us}^*C_1 + \frac{3}{4}V_{tb}V_{ts}^*[2C_3 + \frac{1}{2}C_9]$	$\frac{3}{4}V_{tb}V_{ts}^*[2C_5 + \frac{1}{2}C_7]$
C_{g3}	$-\frac{3}{4}V_{ub}V_{us}^*[C_1 - C_2] + \frac{3}{8}V_{tb}V_{ts}^*[4C_3 - 4C_4 + C_9 - C_{10}]$	$\frac{3}{8}V_{tb}V_{ts}^*[4C_5 - 4C_6 + C_7 - C_8]$
C_{g4}	$\frac{3}{4}V_{ub}V_{us}^*C_2 - \frac{3}{8}V_{tb}V_{ts}^*[4C_4 + C_{10}]$	$-\frac{3}{8}V_{tb}V_{ts}^*[4C_6 + C_8]$
Eq_{g1}	$\frac{3}{4}V_{ub}V_{us}^*C_1 - \frac{3}{8}V_{tb}V_{ts}^*[4C_3 + C_9]$	$-\frac{3}{8}V_{tb}V_{ts}^*[4C_5 + C_7]$
Eq_{g3}	$-\frac{3}{4}V_{ub}V_{us}^*C_2 + \frac{3}{8}V_{tb}V_{ts}^*[4C_4 + C_{10}]$	$\frac{3}{8}V_{tb}V_{ts}^*[4C_6 + C_8]$
$Eq_{g4},\ B_{g1-g4}$	$\frac{3}{4}V_{ub}V_{us}^*[C_1 - C_2] - \frac{3}{8}V_{tb}V_{ts}^*[4C_3 - 4C_4 + C_9 - C_{10}]$	$-\frac{3}{8}V_{tb}V_{ts}^*[4C_5 - 4C_6 + C_7 - C_8]$
$B'_{a1-a4,b1-b4}$	$\frac{1}{4}V_{ub}V_{us}^*[-C_1 + C_2] + \frac{1}{8}V_{tb}V_{ts}^*[4C_3 - 4C_4 + C_9 - C_{10}]$	$\frac{1}{8}V_{tb}V_{ts}^*[4C_5 - 4C_6 + C_7 - C_8]$

TABLE V. Expressions of $[\mathcal{D}b]$ and $\Omega_{R_{ij}}$ for the C, B, and E_q diagrams.

R_{ij}	$[\mathcal{D}b]$	$\Omega_{R_{ij}}$
C_{a1}	$d^2\mathbf{b}_2 d^2\mathbf{b}_3 d^2\mathbf{b}_3' d^2\mathbf{b}_q$	$\frac{1}{(2\pi)^4} K_0(\sqrt{t_A}|\mathbf{b}_2-\mathbf{b}_3|)K_0(\sqrt{t_B}|\mathbf{b}_2-\mathbf{b}_3-\mathbf{b}_3'+\mathbf{b}_q|)K_0(\sqrt{t_C}|\mathbf{b}_2-\mathbf{b}_3'+\mathbf{b}_q|)K_0(\sqrt{t_D}|\mathbf{b}_2+\mathbf{b}_q|)$
C_{a2}	$d^2\mathbf{b}_2 d^2\mathbf{b}_3 d^2\mathbf{b}_3' d^2\mathbf{b}_q$	$\frac{1}{(2\pi)^4} K_0(\sqrt{t_A}|\mathbf{b}_q-\mathbf{b}_3'|)K_0(\sqrt{t_B}|\mathbf{b}_3-\mathbf{b}_2+\mathbf{b}_3'-\mathbf{b}_q|)K_0(\sqrt{t_C}|\mathbf{b}_3|)K_0(\sqrt{t_D}|\mathbf{b}_2+\mathbf{b}_q|)$
C_{a3}	$d^2\mathbf{b}_2 d^2\mathbf{b}_3 d^2\mathbf{b}_q$	$K_0(\sqrt{t_A}|\mathbf{b}_2|)h_2(\mathbf{b}_3-\mathbf{b}_2-\mathbf{b}_q, \mathbf{b}_2+\mathbf{b}_q, t_B, t_C, t_D)$
C_{a4}	$d^2\mathbf{b}_2 d^2\mathbf{b}_3 d^2\mathbf{b}_q$	$K_0(\sqrt{t_B}|\mathbf{b}_3|)h_2(\mathbf{b}_q, \mathbf{b}_2+\mathbf{b}_q, t_A, t_C, t_D)$
C_{a5}	$d^2\mathbf{b}_2 d^2\mathbf{b}_3 d^2\mathbf{b}_2' d^2\mathbf{b}_q$	$\frac{1}{(2\pi)^4} K_0(\sqrt{t_A}|\mathbf{b}_q-\mathbf{b}_2'|)K_0(\sqrt{t_B}|\mathbf{b}_3|)K_0(\sqrt{t_C}|\mathbf{b}_2'|)K_0(\sqrt{t_D}|\mathbf{b}_q+\mathbf{b}_2|)$
C_{a6}	$d^2\mathbf{b}_2 d^2\mathbf{b}_3 d^2\mathbf{b}_2' d^2\mathbf{b}_q$	$\frac{1}{(2\pi)^4} K_0(\sqrt{t_A}|\mathbf{b}_q+\mathbf{b}_2'|)K_0(\sqrt{t_B}|\mathbf{b}_3|)K_0(\sqrt{t_C}|\mathbf{b}_2'|)K_0(\sqrt{t_D}|\mathbf{b}_q+\mathbf{b}_2|)$
C_{a7}	$d^2\mathbf{b}_2 d^2\mathbf{b}_3 d^2\mathbf{b}_3' d^2\mathbf{b}_q$	$\frac{1}{(2\pi)^4} K_0(\sqrt{t_A}|\mathbf{b}_q|)K_0(\sqrt{t_B}|\mathbf{b}_3|)K_0(\sqrt{t_C}|\mathbf{b}_3-\mathbf{b}_2+\mathbf{b}_3'-\mathbf{b}_q|)K_0(\sqrt{t_D}|\mathbf{b}_3+\mathbf{b}_3'|)$
C_{b1}	$d^2\mathbf{b}_2 d^2\mathbf{b}_3 d^2\mathbf{b}_2' d^2\mathbf{b}_3'$	$\frac{1}{(2\pi)^4} K_0(\sqrt{t_A}|\mathbf{b}_2-\mathbf{b}_3|)K_0(\sqrt{t_B}|\mathbf{b}_2'-\mathbf{b}_3'|)K_0(\sqrt{t_C}|\mathbf{b}_3+\mathbf{b}_3'|)K_0(\sqrt{t_D}|\mathbf{b}_2'|)$
C_{b2}	$d^2\mathbf{b}_2 d^2\mathbf{b}_3 d^2\mathbf{b}_2' d^2\mathbf{b}_3'$	$\frac{1}{(2\pi)^4} K_0(\sqrt{t_A}|\mathbf{b}_2+\mathbf{b}_3'|)K_0(\sqrt{t_B}|\mathbf{b}_3+\mathbf{b}_2'|)K_0(\sqrt{t_C}|\mathbf{b}_3+\mathbf{b}_3'|)K_0(\sqrt{t_D}|\mathbf{b}_2'|)$
C_{b3}	$d^2\mathbf{b}_2 d^2\mathbf{b}_3 d^2\mathbf{b}_2' d^2\mathbf{b}_3'$	$\frac{1}{(2\pi)^4} K_0(\sqrt{t_A}|\mathbf{b}_2|)K_0(\sqrt{t_B}|\mathbf{b}_2'-\mathbf{b}_3'|)K_0(\sqrt{t_C}|\mathbf{b}_3+\mathbf{b}_3'|)K_0(\sqrt{t_D}|\mathbf{b}_2'|)$
C_{b4}	$d^2\mathbf{b}_2 d^2\mathbf{b}_3 d^2\mathbf{b}_2'$	$K_0(\sqrt{t_B}|\mathbf{b}_3+\mathbf{b}_2'|)h_2(\mathbf{b}_2, \mathbf{b}_2', t_A, t_C, t_D)$
C_{b5}	$d^2\mathbf{b}_2 d^2\mathbf{b}_3 d^2\mathbf{b}_2'$	$K_0(\sqrt{t_A}|\mathbf{b}_2+\mathbf{b}_2'|)h_2(\mathbf{b}_3+\mathbf{b}_2', \mathbf{b}_2', t_B, t_C, t_D)$
C_{b6}	$d^2\mathbf{b}_2 d^2\mathbf{b}_3 d^2\mathbf{b}_2' d^2\mathbf{b}_3'$	$\frac{1}{(2\pi)^4} K_0(\sqrt{t_A}|\mathbf{b}_3-\mathbf{b}_2+\mathbf{b}_3'|)K_0(\sqrt{t_B}|\mathbf{b}_2'-\mathbf{b}_3'|)K_0(\sqrt{t_C}|\mathbf{b}_3+\mathbf{b}_3'|)K_0(\sqrt{t_D}|\mathbf{b}_2'-\mathbf{b}_3'-\mathbf{b}_3|)$
C_{b7}	$d^2\mathbf{b}_2 d^2\mathbf{b}_3 d^2\mathbf{b}_2' d^2\mathbf{b}_q$	$\frac{1}{(2\pi)^4} K_0(\sqrt{t_A}|\mathbf{b}_q|)K_0(\sqrt{t_B}|\mathbf{b}_3+\mathbf{b}_2'|)K_0(\sqrt{t_C}|\mathbf{b}_2+\mathbf{b}_q|)K_0(\sqrt{t_D}|\mathbf{b}_2'|)$
C_{c1}	$d^2\mathbf{b}_2 d^2\mathbf{b}_3 d^2\mathbf{b}_2' d^2\mathbf{b}_3'$	$\frac{1}{(2\pi)^4} K_0(\sqrt{t_A}|\mathbf{b}_2-\mathbf{b}_3|)K_0(\sqrt{t_B}|\mathbf{b}_3'|)K_0(\sqrt{t_C}|\mathbf{b}_3-\mathbf{b}_2'+\mathbf{b}_3'|)K_0(\sqrt{t_D}|\mathbf{b}_2'|)$
C_{c2}	$d^2\mathbf{b}_2 d^2\mathbf{b}_3 d^2\mathbf{b}_2' d^2\mathbf{b}_3'$	$\frac{1}{(2\pi)^4} K_0(\sqrt{t_A}|\mathbf{b}_2'-\mathbf{b}_3'-\mathbf{b}_2|)K_0(\sqrt{t_B}|\mathbf{b}_3-\mathbf{b}_2'|)K_0(\sqrt{t_C}|\mathbf{b}_3-\mathbf{b}_2'-\mathbf{b}_3'|)K_0(\sqrt{t_D}|\mathbf{b}_2'|)$
C_{c3}	$d^2\mathbf{b}_2 d^2\mathbf{b}_3 d^2\mathbf{b}_2' d^2\mathbf{b}_3'$	$\frac{1}{(2\pi)^4} K_0(\sqrt{t_A}|\mathbf{b}_2|)K_0(\sqrt{t_B}|\mathbf{b}_3'|)K_0(\sqrt{t_C}|\mathbf{b}_2'-\mathbf{b}_3'-\mathbf{b}_3|)K_0(\sqrt{t_D}|\mathbf{b}_2'|)$
C_{c4}	$d^2\mathbf{b}_2 d^2\mathbf{b}_3 d^2\mathbf{b}_2' d^2\mathbf{b}_3'$	$\frac{1}{(2\pi)^4} K_0(\sqrt{t_A}|\mathbf{b}_2-\mathbf{b}_3+\mathbf{b}_2'-\mathbf{b}_3'|)K_0(\sqrt{t_B}|\mathbf{b}_3'|)K_0(\sqrt{t_C}|\mathbf{b}_2'-\mathbf{b}_3'-\mathbf{b}_3|)K_0(\sqrt{t_D}|\mathbf{b}_3+\mathbf{b}_3'|)$
C_{c5}	$d^2\mathbf{b}_2 d^2\mathbf{b}_3 d^2\mathbf{b}_2'$	$K_0(\sqrt{t_B}|\mathbf{b}_3-\mathbf{b}_2'|)h_2(\mathbf{b}_2, \mathbf{b}_2', t_A, t_C, t_D)$
C_{c6}	$d^2\mathbf{b}_2 d^2\mathbf{b}_3 d^2\mathbf{b}_2'$	$K_0(\sqrt{t_A}|\mathbf{b}_2-\mathbf{b}_2'|)h_2(\mathbf{b}_3-\mathbf{b}_2', \mathbf{b}_2', t_B, t_C, t_D)$
C_{c7}	$d^2\mathbf{b}_2 d^2\mathbf{b}_3 d^2\mathbf{b}_2' d^2\mathbf{b}_q$	$\frac{1}{(2\pi)^4} K_0(\sqrt{t_A}|\mathbf{b}_q|)K_0(\sqrt{t_B}|\mathbf{b}_3-\mathbf{b}_2'|)K_0(\sqrt{t_C}|\mathbf{b}_2+\mathbf{b}_q|)K_0(\sqrt{t_D}|\mathbf{b}_2'|)$
C_{d1}	$d^2\mathbf{b}_2 d^2\mathbf{b}_3 d^2\mathbf{b}_3' d^2\mathbf{b}_q$	$\frac{1}{(2\pi)^4} K_0(\sqrt{t_A}|\mathbf{b}_2-\mathbf{b}_3|)K_0(\sqrt{t_B}|\mathbf{b}_2+\mathbf{b}_3'+\mathbf{b}_q|)K_0(\sqrt{t_C}|\mathbf{b}_3+\mathbf{b}_3'|)K_0(\sqrt{t_D}|\mathbf{b}_2+\mathbf{b}_q|)$
C_{d2}	$d^2\mathbf{b}_2 d^2\mathbf{b}_3 d^2\mathbf{b}_3' d^2\mathbf{b}_q$	$\frac{1}{(2\pi)^4} K_0(\sqrt{t_A}|\mathbf{b}_2+\mathbf{b}_3'|)K_0(\sqrt{t_B}|\mathbf{b}_2-\mathbf{b}_3+\mathbf{b}_q|)K_0(\sqrt{t_C}|\mathbf{b}_3+\mathbf{b}_3'|)K_0(\sqrt{t_D}|\mathbf{b}_2+\mathbf{b}_q|)$
C_{d3}	$d^2\mathbf{b}_2 d^2\mathbf{b}_3 d^2\mathbf{b}_3' d^2\mathbf{b}_q$	$\frac{1}{(2\pi)^4} K_0(\sqrt{t_A}|\mathbf{b}_2|)K_0(\sqrt{t_B}|\mathbf{b}_2-\mathbf{b}_3+\mathbf{b}_q|)K_0(\sqrt{t_C}|\mathbf{b}_3+\mathbf{b}_3'|)K_0(\sqrt{t_D}|\mathbf{b}_3-\mathbf{b}_2+\mathbf{b}_3'-\mathbf{b}_q|)$
C_{d4}	$d^2\mathbf{b}_2 d^2\mathbf{b}_3 d^2\mathbf{b}_2' d^2\mathbf{b}_q$	$\frac{1}{(2\pi)^4} K_0(\sqrt{t_A}|\mathbf{b}_2+\mathbf{b}_2'|)K_0(\sqrt{t_B}|\mathbf{b}_2-\mathbf{b}_3+\mathbf{b}_q|)K_0(\sqrt{t_C}|\mathbf{b}_2'|)K_0(\sqrt{t_D}|\mathbf{b}_2+\mathbf{b}_q|)$
C_{d5}	$d^2\mathbf{b}_2 d^2\mathbf{b}_3 d^2\mathbf{b}_2' d^2\mathbf{b}_q$	$\frac{1}{(2\pi)^4} K_0(\sqrt{t_A}|\mathbf{b}_2-\mathbf{b}_2'|)K_0(\sqrt{t_B}|\mathbf{b}_2-\mathbf{b}_3+\mathbf{b}_q|)K_0(\sqrt{t_C}|\mathbf{b}_2'|)K_0(\sqrt{t_D}|\mathbf{b}_2+\mathbf{b}_q|)$
C_{d6}	$d^2\mathbf{b}_2 d^2\mathbf{b}_3 d^2\mathbf{b}_q$	$K_0(\sqrt{t_B}|\mathbf{b}_2-\mathbf{b}_3+\mathbf{b}_q|)h_2(\mathbf{b}_2, \mathbf{b}_2+\mathbf{b}_q, t_A, t_C, t_D)$
C_{d7}	$d^2\mathbf{b}_2 d^2\mathbf{b}_3 d^2\mathbf{b}_q$	$K_0(\sqrt{t_A}|\mathbf{b}_q|)h_2(\mathbf{b}_3-\mathbf{b}_2-\mathbf{b}_q, \mathbf{b}_2+\mathbf{b}_q, t_B, t_C, t_D)$
C_{e1}	$d^2\mathbf{b}_2 d^2\mathbf{b}_3 d^2\mathbf{b}_3' d^2\mathbf{b}_q$	$\frac{1}{(2\pi)^4} K_0(\sqrt{t_A}|\mathbf{b}_2-\mathbf{b}_3|)K_0(\sqrt{t_B}|\mathbf{b}_q-\mathbf{b}_3-\mathbf{b}_3'|)K_0(\sqrt{t_C}|\mathbf{b}_2-\mathbf{b}_3-\mathbf{b}_3'+\mathbf{b}_q|)K_0(\sqrt{t_D}|\mathbf{b}_3+\mathbf{b}_3'|)$
C_{e2}	$d^2\mathbf{b}_2 d^2\mathbf{b}_3 d^2\mathbf{b}_2' d^2\mathbf{b}_q$	$\frac{1}{(2\pi)^4} K_0(\sqrt{t_A}|\mathbf{b}_2-\mathbf{b}_3|)K_0(\sqrt{t_B}|\mathbf{b}_q-\mathbf{b}_2'|)K_0(\sqrt{t_C}|\mathbf{b}_2+\mathbf{b}_q|)K_0(\sqrt{t_D}|\mathbf{b}_2'|)$
C_{e3}	$d^2\mathbf{b}_2 d^2\mathbf{b}_3 d^2\mathbf{b}_2' d^2\mathbf{b}_q$	$\frac{1}{(2\pi)^4} K_0(\sqrt{t_A}|\mathbf{b}_2-\mathbf{b}_3|)K_0(\sqrt{t_B}|\mathbf{b}_2'+\mathbf{b}_q|)K_0(\sqrt{t_C}|\mathbf{b}_2'|)K_0(\sqrt{t_D}|\mathbf{b}_3-\mathbf{b}_2'+\mathbf{b}_3'|)$
C_{e4}	$d^2\mathbf{b}_2' d^2\mathbf{b}_3' d^2\mathbf{b}_q$	$K_0(\sqrt{t_A}|\mathbf{b}_2+\mathbf{b}_3'|)K_0(\sqrt{t_B}|\mathbf{b}_q|)h_1(\mathbf{b}_2+\mathbf{b}_q, t_C, t_D)$
C_{f1}	$d^2\mathbf{b}_2 d^2\mathbf{b}_3 d^2\mathbf{b}_3' d^2\mathbf{b}_q$	$\frac{1}{(2\pi)^4} K_0(\sqrt{t_A}|\mathbf{b}_q-\mathbf{b}_3'|)K_0(\sqrt{t_B}|\mathbf{b}_2|)K_0(\sqrt{t_C}|\mathbf{b}_2-\mathbf{b}_3-\mathbf{b}_3'+\mathbf{b}_q|)K_0(\sqrt{t_D}|\mathbf{b}_3+\mathbf{b}_3'|)$
C_{f2}	$d^2\mathbf{b}_2 d^2\mathbf{b}_3 d^2\mathbf{b}_2' d^2\mathbf{b}_q$	$\frac{1}{(2\pi)^4} K_0(\sqrt{t_A}|\mathbf{b}_3+\mathbf{b}_q|)K_0(\sqrt{t_B}|\mathbf{b}_2+\mathbf{b}_2'|)K_0(\sqrt{t_C}|\mathbf{b}_2+\mathbf{b}_q|)K_0(\sqrt{t_D}|\mathbf{b}_2'|)$
C_{f3}	$d^2\mathbf{b}_2 d^2\mathbf{b}_3 d^2\mathbf{b}_2' d^2\mathbf{b}_q$	$\frac{1}{(2\pi)^4} K_0(\sqrt{t_A}|\mathbf{b}_3+\mathbf{b}_q|)K_0(\sqrt{t_B}|\mathbf{b}_2-\mathbf{b}_2'|)K_0(\sqrt{t_C}|\mathbf{b}_2+\mathbf{b}_q|)K_0(\sqrt{t_D}|\mathbf{b}_2'|)$
C_{f4}	$d^2\mathbf{b}_2 d^2\mathbf{b}_3 d^2\mathbf{b}_q$	$h_3(\mathbf{b}_q-\mathbf{b}_2+\mathbf{b}_3, \mathbf{b}_q, \mathbf{b}_2, t_A, t_B, t_C, t_D)$
C_{g1}	$d^2\mathbf{b}_2 d^2\mathbf{b}_3 d^2\mathbf{b}_q$	$K_0(\sqrt{t_D}|\mathbf{b}_2+\mathbf{b}_q|)h_2(\mathbf{b}_2-\mathbf{b}_3, \mathbf{b}_2-\mathbf{b}_3-\mathbf{b}_3'+\mathbf{b}_q, t_A, t_B, t_C)$
C_{g2}	$d^2\mathbf{b}_2 d^2\mathbf{b}_3 d^2\mathbf{b}_3'$	$K_0(\sqrt{t_D}|\mathbf{b}_3+\mathbf{b}_3'|)h_2(\mathbf{b}_2, \mathbf{b}_3, t_A, t_B, t_C)$
C_{g3}	$d^2\mathbf{b}_2 d^2\mathbf{b}_3' d^2\mathbf{b}_q$	$K_0(\sqrt{t_D}|\mathbf{b}_2+\mathbf{b}_q|)h_2(\mathbf{b}_q, \mathbf{b}_2+\mathbf{b}_3'+\mathbf{b}_q, t_A, t_B, t_C)$
C_{g4}	$d^2\mathbf{b}_2' d^2\mathbf{b}_3' d^2\mathbf{b}_q$	$K_0(\sqrt{t_D}|\mathbf{b}_2'|)h_2(\mathbf{b}_2'+\mathbf{b}_q, \mathbf{b}_3', t_A, t_B, t_C)$
Eq_{a1}	$d^2\mathbf{b}_2 d^2\mathbf{b}_3 d^2\mathbf{b}_3' d^2\mathbf{b}_q$	$\frac{1}{(2\pi)^4} K_0(\sqrt{t_A}|\mathbf{b}_2-\mathbf{b}_3|)K_0(\sqrt{t_B}|\mathbf{b}_3+\mathbf{b}_3'-\mathbf{b}_q|)K_0(\sqrt{t_C}|\mathbf{b}_2|)K_0(\sqrt{t_D}|\mathbf{b}_3+\mathbf{b}_3'|)$
Eq_{a2}	$d^2\mathbf{b}_3 d^2\mathbf{b}_3' d^2\mathbf{b}_q$	$K_0(\sqrt{t_B}|\mathbf{b}_3+\mathbf{b}_3'-\mathbf{b}_q|)h_2(\mathbf{b}_3', \mathbf{b}_3+\mathbf{b}_3', t_A, t_C, t_D)$
Eq_{a3}	$d^2\mathbf{b}_3 d^2\mathbf{b}_3' d^2\mathbf{b}_q$	$K_0(\sqrt{t_A}|\mathbf{b}_3'|)h_2(\mathbf{b}_3+\mathbf{b}_3', \mathbf{b}_q, t_B, t_C, t_D)$
Eq_{a4}	$d^2\mathbf{b}_2 d^2\mathbf{b}_3 d^2\mathbf{b}_3' d^2\mathbf{b}_q$	$\frac{1}{(2\pi)^4} K_0(\sqrt{t_A}|\mathbf{b}_3|)K_0(\sqrt{t_B}|\mathbf{b}_2-\mathbf{b}_3-\mathbf{b}_3'+\mathbf{b}_q|)K_0(\sqrt{t_C}|\mathbf{b}_2|)K_0(\sqrt{t_D}|\mathbf{b}_2-\mathbf{b}_3-\mathbf{b}_3'|)$

(Table continued)

TABLE V. *(Continued)*

R_{ij}	$[\mathcal{D}b]$	$\Omega_{R_{ij}}$
Eq_{a5}	$d^2\mathbf{b}_2 d^2\mathbf{b}_3 d^2\mathbf{b}'_3 d^2\mathbf{b}_q$	$\frac{1}{(2\pi)^4} K_0(\sqrt{t_A}\|\mathbf{b}'_2 - \mathbf{b}'_3 + \mathbf{b}_q\|) K_0(\sqrt{t_B}\|\mathbf{b}'_2\|) K_0(\sqrt{t_C}\|\mathbf{b}_3 - \mathbf{b}'_2 + \mathbf{b}'_3 - \mathbf{b}_q\|) K_0(\sqrt{t_D}\|\mathbf{b}_3 + \mathbf{b}'_3\|)$
Eq_{a6}	$d^2\mathbf{b}_3 d^2\mathbf{b}'_2 d^2\mathbf{b}'_3 d^2\mathbf{b}_q$	$\frac{1}{(2\pi)^4} K_0(\sqrt{t_A}\|\mathbf{b}_3 - \mathbf{b}_q\|) K_0(\sqrt{t_B}\|\mathbf{b}'_2\|) K_0(\sqrt{t_C}\|\mathbf{b}_3 - \mathbf{b}'_2 - \mathbf{b}'_3 - \mathbf{b}_q\|) K_0(\sqrt{t_D}\|\mathbf{b}_3 + \mathbf{b}'_3\|)$
Eq_{a7}	$d^2\mathbf{b}_3 d^2\mathbf{b}'_2 d^2\mathbf{b}'_3 d^2\mathbf{b}_q$	$\frac{1}{(2\pi)^4} K_0(\sqrt{t_A}\|\mathbf{b}'_2 - \mathbf{b}'_3\|) K_0(\sqrt{t_B}\|\mathbf{b}_3 + \mathbf{b}'_3 - \mathbf{b}_q\|) K_0(\sqrt{t_C}\|\mathbf{b}_3 - \mathbf{b}'_2 + \mathbf{b}'_3 - \mathbf{b}_q\|) K_0(\sqrt{t_D}\|\mathbf{b}_3 + \mathbf{b}'_3\|)$
Eq_{b1}	$d^2\mathbf{b}_2 d^2\mathbf{b}_3 d^2\mathbf{b}_q$	$K_0(\sqrt{t_A}\|\mathbf{b}_2 - \mathbf{b}_3\|) h_2(\mathbf{b}_q, \mathbf{b}_2 - \mathbf{b}_3, t_B, t_C, t_D)$
Eq_{b2}	$d^2\mathbf{b}_2 d^2\mathbf{b}_3 d^2\mathbf{b}_q$	$K_0(\sqrt{t_B}\|\mathbf{b}_2 - \mathbf{b}_q\|) h_2(\mathbf{b}_3, \mathbf{b}_2, t_A, t_C, t_D)$
Eq_{b3}	$d^2\mathbf{b}_2 d^2\mathbf{b}_3 d^2\mathbf{b}'_2 d^2\mathbf{b}_q$	$\frac{1}{(2\pi)^4} K_0(\sqrt{t_A}\|\mathbf{b}_3 - \mathbf{b}'_2 - \mathbf{b}_q\|) K_0(\sqrt{t_B}\|\mathbf{b}_2 - \mathbf{b}_q\|) K_0(\sqrt{t_C}\|\mathbf{b}'_2 + \mathbf{b}_q\|) K_0(\sqrt{t_D}\|\mathbf{b}_2\|)$
Eq_{b4}	$d^2\mathbf{b}_2 d^2\mathbf{b}_3 d^2\mathbf{b}'_3 d^2\mathbf{b}_q$	$\frac{1}{(2\pi)^4} K_0(\sqrt{t_A}\|\mathbf{b}_3\|) K_0(\sqrt{t_B}\|\mathbf{b}_2 - \mathbf{b}_3 - \mathbf{b}'_3 - \mathbf{b}_q\|) K_0(\sqrt{t_C}\|\mathbf{b}_3 + \mathbf{b}'_3\|) K_0(\sqrt{t_D}\|\mathbf{b}_2 - \mathbf{b}_3 - \mathbf{b}'_3\|)$
Eq_{b5}	$d^2\mathbf{b}_2 d^2\mathbf{b}_3 d^2\mathbf{b}'_2 d^2\mathbf{b}_q$	$\frac{1}{(2\pi)^4} K_0(\sqrt{t_A}\|\mathbf{b}_3 + \mathbf{b}'_2 + \mathbf{b}_q\|) K_0(\sqrt{t_B}\|\mathbf{b}_2 + \mathbf{b}'_2\|) K_0(\sqrt{t_C}\|\mathbf{b}'_2 + \mathbf{b}_q\|) K_0(\sqrt{t_D}\|\mathbf{b}_2\|)$
Eq_{b6}	$d^2\mathbf{b}_2 d^2\mathbf{b}_3 d^2\mathbf{b}'_2 d^2\mathbf{b}_q$	$\frac{1}{(2\pi)^4} K_0(\sqrt{t_A}\|\mathbf{b}_3 - \mathbf{b}_q\|) K_0(\sqrt{t_B}\|\mathbf{b}_2 + \mathbf{b}'_2\|) K_0(\sqrt{t_C}\|\mathbf{b}'_2 + \mathbf{b}_q\|) K_0(\sqrt{t_D}\|\mathbf{b}_2\|)$
Eq_{b7}	$d^2\mathbf{b}_2 d^2\mathbf{b}_3 d^2\mathbf{b}'_2 d^2\mathbf{b}_q$	$\frac{1}{(2\pi)^4} K_0(\sqrt{t_A}\|\mathbf{b}_3 + \mathbf{b}'_2\|) K_0(\sqrt{t_B}\|\mathbf{b}_2 - \mathbf{b}_q\|) K_0(\sqrt{t_C}\|\mathbf{b}'_2 + \mathbf{b}_q\|) K_0(\sqrt{t_D}\|\mathbf{b}_2\|)$
Eq_{c1}	$d^2\mathbf{b}_2 d^2\mathbf{b}_3 d^2\mathbf{b}'_3 d^2\mathbf{b}_q$	$\frac{1}{(2\pi)^4} K_0(\sqrt{t_A}\|\mathbf{b}_2 - \mathbf{b}_3\|) K_0(\sqrt{t_B}\|\mathbf{b}_3 + \mathbf{b}'_3 - \mathbf{b}_q\|) K_0(\sqrt{t_C}\|\mathbf{b}_2 - \mathbf{b}_3 - \mathbf{b}'_3\|) K_0(\sqrt{t_D}\|\mathbf{b}_3 + \mathbf{b}'_3\|)$
Eq_{c2}	$d^2\mathbf{b}_2 d^2\mathbf{b}_3 d^2\mathbf{b}'_3 d^2\mathbf{b}_q$	$\frac{1}{(2\pi)^4} K_0(\sqrt{t_A}\|\mathbf{b}'_3\|) K_0(\sqrt{t_B}\|\mathbf{b}_2 - \mathbf{b}_q\|) K_0(\sqrt{t_C}\|\mathbf{b}_2 - \mathbf{b}_3 - \mathbf{b}'_3\|) K_0(\sqrt{t_D}\|\mathbf{b}_2\|)$
Eq_{c3}	$d^2\mathbf{b}_3 d^2\mathbf{b}'_2 d^2\mathbf{b}'_3$	$K_0(\sqrt{t_A}\|\mathbf{b}_3\|) h_2(\mathbf{b}'_2, \mathbf{b}_3 + \mathbf{b}'_3, t_B, t_C, t_D)$
Eq_{c4}	$d^2\mathbf{b}_3 d^2\mathbf{b}'_2 d^2\mathbf{b}'_3$	$K_0(\sqrt{t_B}\|\mathbf{b}_3 - \mathbf{b}'_2 + \mathbf{b}'_3\|) h_2(\mathbf{b}'_3, \mathbf{b}_3 + \mathbf{b}'_3, t_A, t_C, t_D)$
Eq_{c5}	$d^2\mathbf{b}_3 d^2\mathbf{b}'_2 d^2\mathbf{b}'_3 d^2\mathbf{b}_q$	$\frac{1}{(2\pi)^4} K_0(\sqrt{t_A}\|\mathbf{b}'_2 - \mathbf{b}'_3 + \mathbf{b}_q\|) K_0(\sqrt{t_B}\|\mathbf{b}'_2 - \mathbf{b}_3 - \mathbf{b}'_3\|) K_0(\sqrt{t_C}\|\mathbf{b}'_2 + \mathbf{b}_q\|) K_0(\sqrt{t_D}\|\mathbf{b}_3 + \mathbf{b}'_3\|)$
Eq_{c6}	$d^2\mathbf{b}_3 d^2\mathbf{b}'_2 d^2\mathbf{b}'_3 d^2\mathbf{b}_q$	$\frac{1}{(2\pi)^4} K_0(\sqrt{t_A}\|\mathbf{b}'_3 + \mathbf{b}_q\|) K_0(\sqrt{t_B}\|\mathbf{b}_3 - \mathbf{b}'_2 + \mathbf{b}'_3\|) K_0(\sqrt{t_C}\|\mathbf{b}'_2 + \mathbf{b}_q\|) K_0(\sqrt{t_D}\|\mathbf{b}_3 + \mathbf{b}'_3\|)$
Eq_{c7}	$d^2\mathbf{b}_3 d^2\mathbf{b}'_2 d^2\mathbf{b}'_3 d^2\mathbf{b}_q$	$\frac{1}{(2\pi)^4} K_0(\sqrt{t_A}\|\mathbf{b}'_2 - \mathbf{b}'_3\|) K_0(\sqrt{t_B}\|\mathbf{b}_3 - \mathbf{b}'_3 + \mathbf{b}_q\|) K_0(\sqrt{t_C}\|\mathbf{b}'_2 + \mathbf{b}_q\|) K_0(\sqrt{t_D}\|\mathbf{b}_3 + \mathbf{b}'_3\|)$
Eq_{d1}	$d^2\mathbf{b}_2 d^2\mathbf{b}_3 d^2\mathbf{b}'_2 d^2\mathbf{b}_q$	$\frac{1}{(2\pi)^4} K_0(\sqrt{t_A}\|\mathbf{b}_2 - \mathbf{b}_3\|) K_0(\sqrt{t_B}\|\mathbf{b}_q\|) K_0(\sqrt{t_C}\|\mathbf{b}_2\|) K_0(\sqrt{t_D}\|\mathbf{b}'_2 + \mathbf{b}_q\|)$
Eq_{d2}	$d^2\mathbf{b}_3 d^2\mathbf{b}'_2 d^2\mathbf{b}'_3 d^2\mathbf{b}_q$	$\frac{1}{(2\pi)^4} K_0(\sqrt{t_A}\|\mathbf{b}'_3\|) K_0(\sqrt{t_B}\|\mathbf{b}_q\|) K_0(\sqrt{t_C}\|\mathbf{b}_3 + \mathbf{b}'_3\|) K_0(\sqrt{t_D}\|\mathbf{b}_3 - \mathbf{b}'_2 + \mathbf{b}'_3 - \mathbf{b}_q\|)$
Eq_{d3}	$d^2\mathbf{b}_3 d^2\mathbf{b}'_2 d^2\mathbf{b}'_3 d^2\mathbf{b}_q$	$\frac{1}{(2\pi)^4} K_0(\sqrt{t_A}\|\mathbf{b}_3\|) K_0(\sqrt{t_B}\|\mathbf{b}_q\|) K_0(\sqrt{t_C}\|\mathbf{b}_3 + \mathbf{b}'_3\|) K_0(\sqrt{t_D}\|\mathbf{b}'_2 + \mathbf{b}_q\|)$
Eq_{d4}	$d^2\mathbf{b}'_2 d^2\mathbf{b}'_3 d^2\mathbf{b}_q$	$K_0(\sqrt{t_B}\|\mathbf{b}_q\|) h_2(\mathbf{b}'_2 - \mathbf{b}'_3 + \mathbf{b}_q, \mathbf{b}'_2 - \mathbf{b}_q, t_A, t_C, t_D)$
Eq_{d5}	$d^2\mathbf{b}'_2 d^2\mathbf{b}'_3 d^2\mathbf{b}_q$	$K_0(\sqrt{t_A}\|\mathbf{b}'_2 - \mathbf{b}'_3 + \mathbf{b}_q\|) h_2(\mathbf{b}'_2, \mathbf{b}'_2 + \mathbf{b}_q, t_B, t_C, t_D)$
Eq_{d6}	$d^2\mathbf{b}'_2 d^2\mathbf{b}'_3 d^2\mathbf{b}_q$	$h_3(\mathbf{b}'_3 - \mathbf{b}_q, \mathbf{b}'_2, \mathbf{b}'_2 - \mathbf{b}_q, t_A, t_B, t_C, t_D)$
Eq_{d7}	$d^2\mathbf{b}'_2 d^2\mathbf{b}'_3 d^2\mathbf{b}_q$	$K_0(\sqrt{t_A}\|\mathbf{b}_2 - \mathbf{b}'_3\|) K_0(\sqrt{t_B}\|\mathbf{b}_q\|) h_1(\mathbf{b}'_2 + \mathbf{b}_q, t_C, t_D)$
Eq_{e1}	$d^2\mathbf{b}_2 d^2\mathbf{b}_3 d^2\mathbf{b}'_3 d^2\mathbf{b}_q$	$\frac{1}{(2\pi)^4} K_0(\sqrt{t_A}\|\mathbf{b}_3 + \mathbf{b}_q\|) K_0(\sqrt{t_B}\|\mathbf{b}_2 - \mathbf{b}_3\|) K_0(\sqrt{t_C}\|\mathbf{b}_3 + \mathbf{b}'_3\|) K_0(\sqrt{t_D}\|\mathbf{b}_2\|)$
Eq_{e2}	$d^2\mathbf{b}_3 d^2\mathbf{b}'_2 d^2\mathbf{b}'_3 d^2\mathbf{b}_q$	$\frac{1}{(2\pi)^4} K_0(\sqrt{t_A}\|\mathbf{b}_3 - \mathbf{b}_q\|) K_0(\sqrt{t_B}\|\mathbf{b}'_3\|) K_0(\sqrt{t_C}\|\mathbf{b}_3 - \mathbf{b}'_2 + \mathbf{b}'_3 - \mathbf{b}_q\|) K_0(\sqrt{t_D}\|\mathbf{b}'_2 + \mathbf{b}_q\|)$
Eq_{e3}	$d^2\mathbf{b}_2 d^2\mathbf{b}_3 d^2\mathbf{b}'_3 d^2\mathbf{b}_q$	$\frac{1}{(2\pi)^4} K_0(\sqrt{t_A}\|\mathbf{b}'_3 + \mathbf{b}_q\|) K_0(\sqrt{t_B}\|\mathbf{b}_3\|) K_0(\sqrt{t_C}\|\mathbf{b}_2 - \mathbf{b}_3 - \mathbf{b}'_3\|) K_0(\sqrt{t_D}\|\mathbf{b}_2\|)$
Eq_{e4}	$d^2\mathbf{b}_3 d^2\mathbf{b}'_2 d^2\mathbf{b}'_3 d^2\mathbf{b}_q$	$\frac{1}{(2\pi)^4} K_0(\sqrt{t_A}\|\mathbf{b}'_2 - \mathbf{b}'_3\|) K_0(\sqrt{t_B}\|\mathbf{b}_3 + \mathbf{b}'_2 + \mathbf{b}_q\|) K_0(\sqrt{t_C}\|\mathbf{b}_3 + \mathbf{b}'_3\|) K_0(\sqrt{t_D}\|\mathbf{b}'_2 + \mathbf{b}_q\|)$
Eq_{f1}	$d^2\mathbf{b}_2 d^2\mathbf{b}_3 d^2\mathbf{b}'_3 d^2\mathbf{b}_q$	$\frac{1}{(2\pi)^4} K_0(\sqrt{t_A}\|\mathbf{b}_3 - \mathbf{b}_q\|) K_0(\sqrt{t_B}\|\mathbf{b}_2 + \mathbf{b}'_3\|) K_0(\sqrt{t_C}\|\mathbf{b}_3 + \mathbf{b}'_3\|) K_0(\sqrt{t_D}\|\mathbf{b}_2\|)$
Eq_{f2}	$d^2\mathbf{b}_3 d^2\mathbf{b}'_2 d^2\mathbf{b}'_3 d^2\mathbf{b}_q$	$\frac{1}{(2\pi)^4} K_0(\sqrt{t_A}\|\mathbf{b}_3 - \mathbf{b}_q\|) K_0(\sqrt{t_B}\|\mathbf{b}'_3\|) K_0(\sqrt{t_C}\|\mathbf{b}_3 - \mathbf{b}'_2 + \mathbf{b}'_3 - \mathbf{b}_q\|) K_0(\sqrt{t_D}\|\mathbf{b}'_2 + \mathbf{b}_q\|)$
Eq_{f3}	$d^2\mathbf{b}_2 d^2\mathbf{b}_3 d^2\mathbf{b}'_3 d^2\mathbf{b}_q$	$\frac{1}{(2\pi)^4} K_0(\sqrt{t_A}\|\mathbf{b}_2 - \mathbf{b}_3 + \mathbf{b}_q\|) K_0(\sqrt{t_B}\|\mathbf{b}_2 - \mathbf{b}'_3\|) K_0(\sqrt{t_C}\|\mathbf{b}_2 - \mathbf{b}_3 - \mathbf{b}'_3\|) K_0(\sqrt{t_D}\|\mathbf{b}_2\|)$
Eq_{f4}	$d^2\mathbf{b}_3 d^2\mathbf{b}'_2 d^2\mathbf{b}'_3 d^2\mathbf{b}_q$	$\frac{1}{(2\pi)^4} K_0(\sqrt{t_A}\|\mathbf{b}_3 + \mathbf{b}'_2\|) K_0(\sqrt{t_B}\|\mathbf{b}'_2 - \mathbf{b}'_3 + \mathbf{b}_q\|) K_0(\sqrt{t_C}\|\mathbf{b}_3 + \mathbf{b}'_3\|) K_0(\sqrt{t_D}\|\mathbf{b}'_2 + \mathbf{b}_q\|)$
Eq_{g1}	$d^2\mathbf{b}_2 d^2\mathbf{b}'_3 d^2\mathbf{b}_q$	$K_0(\sqrt{t_D}\|\mathbf{b}_2\|) h_2(\mathbf{b}_2 - \mathbf{b}_q, \mathbf{b}_2 + \mathbf{b}_q, t_A, t_B, t_C)$
Eq_{g2}	$d^2\mathbf{b}_3 d^2\mathbf{b}'_2 d^2\mathbf{b}_q$	$K_0(\sqrt{t_D}\|\mathbf{b}'_2 + \mathbf{b}_q\|) h_2(\mathbf{b}'_2, \mathbf{b}_3 - \mathbf{b}'_2 - \mathbf{b}_q, t_A, t_B, t_C)$
Eq_{g3}	$d^2\mathbf{b}_2 d^2\mathbf{b}'_3 d^2\mathbf{b}_q$	$K_0(\sqrt{t_D}\|\mathbf{b}_2\|) h_2(\mathbf{b}_2 + \mathbf{b}_q, \mathbf{b}_2 - \mathbf{b}'_3, t_A, t_B, t_C)$
Eq_{g4}	$d^2\mathbf{b}'_2 d^2\mathbf{b}'_3 d^2\mathbf{b}_q$	$K_0(\sqrt{t_D}\|\mathbf{b}'_2 + \mathbf{b}_q\|) h_2(\mathbf{b}_q, \mathbf{b}'_2 - \mathbf{b}'_3 + \mathbf{b}_q, t_A, t_B, t_C)$
B_{a1}	$d^2\mathbf{b}_2 d^2\mathbf{b}_3 d^2\mathbf{b}'_3 d^2\mathbf{b}_q$	$\frac{1}{(2\pi)^4} K_0(\sqrt{t_A}\|\mathbf{b}_3\|) K_0(\sqrt{t_B}\|\mathbf{b}'_3\|) K_0(\sqrt{t_C}\|\mathbf{b}_2\|) K_0(\sqrt{t_D}\|\mathbf{b}_2 - \mathbf{b}_3 - \mathbf{b}'_3 - \mathbf{b}_q\|)$
B_{a2}	$d^2\mathbf{b}_3 d^2\mathbf{b}'_2 d^2\mathbf{b}'_3 d^2\mathbf{b}_q$	$\frac{1}{(2\pi)^4} K_0(\sqrt{t_A}\|\mathbf{b}'_2 - \mathbf{b}'_3 - \mathbf{b}_q\|) K_0(\sqrt{t_B}\|\mathbf{b}'_3\|) K_0(\sqrt{t_C}\|\mathbf{b}_3 - \mathbf{b}'_2 + \mathbf{b}'_3 + \mathbf{b}_q\|) K_0(\sqrt{t_D}\|\mathbf{b}_3 + \mathbf{b}'_3 + \mathbf{b}_q\|)$
B_{a3}	$d^2\mathbf{b}_3 d^2\mathbf{b}'_2 d^2\mathbf{b}'_3 d^2\mathbf{b}_q$	$\frac{1}{(2\pi)^4} K_0(\sqrt{t_A}\|\mathbf{b}_2 - \mathbf{b}_3\|) K_0(\sqrt{t_B}\|\mathbf{b}'_3\|) K_0(\sqrt{t_C}\|\mathbf{b}_2\|) K_0(\sqrt{t_D}\|\mathbf{b}'_2\|)$
B_{a4}	$d^2\mathbf{b}_3 d^2\mathbf{b}'_2 d^2\mathbf{b}'_3$	$K_0(\sqrt{t_B}\|\mathbf{b}'_3\|) h_2(\mathbf{b}'_2 - \mathbf{b}_3, \mathbf{b}'_2, t_A, t_C, t_D)$
B_{a5}	$d^2\mathbf{b}_3 d^2\mathbf{b}'_2 d^2\mathbf{b}'_3$	$K_0(\sqrt{t_A}\|\mathbf{b}_3 - \mathbf{b}'_2\|) h_2(\mathbf{b}'_2 - \mathbf{b}'_3, \mathbf{b}'_2, t_B, t_C, t_D)$
B_{a6}	$d^2\mathbf{b}_3 d^2\mathbf{b}'_2 d^2\mathbf{b}'_3 d^2\mathbf{b}_q$	$\frac{1}{(2\pi)^4} K_0(\sqrt{t_A}\|\mathbf{b}_3 - \mathbf{b}'_2 + \mathbf{b}'_3\|) K_0(\sqrt{t_B}\|\mathbf{b}_3 - \mathbf{b}'_2 + \mathbf{b}_q\|) K_0(\sqrt{t_C}\|\mathbf{b}_3 - \mathbf{b}'_2 + \mathbf{b}'_3 + \mathbf{b}_q\|) K_0(\sqrt{t_D}\|\mathbf{b}'_2\|)$
B_{a7}	$d^2\mathbf{b}_3 d^2\mathbf{b}'_2 d^2\mathbf{b}'_3 d^2\mathbf{b}_q$	$\frac{1}{(2\pi)^4} K_0(\sqrt{t_A}\|\mathbf{b}_q\|) K_0(\sqrt{t_B}\|\mathbf{b}'_3\|) K_0(\sqrt{t_C}\|\mathbf{b}_3 - \mathbf{b}'_2 + \mathbf{b}'_3 - \mathbf{b}_q\|) K_0(\sqrt{t_D}\|\mathbf{b}'_2\|)$
B_{b1}	$d^2\mathbf{b}_2 d^2\mathbf{b}_3 d^2\mathbf{b}'_3 d^2\mathbf{b}_q$	$\frac{1}{(2\pi)^4} K_0(\sqrt{t_A}\|\mathbf{b}_3\|) K_0(\sqrt{t_B}\|\mathbf{b}_2 - \mathbf{b}_3 - \mathbf{b}_q\|) K_0(\sqrt{t_C}\|\mathbf{b}_3 + \mathbf{b}'_3 + \mathbf{b}_q\|) K_0(\sqrt{t_D}\|\mathbf{b}_2 - \mathbf{b}_3 - \mathbf{b}'_3 - \mathbf{b}_q\|)$

(Table continued)

TABLE V. *(Continued)*

R_{ij}	$[\mathcal{D}b]$	$\Omega_{R_{ij}}$
B_{b2}	$d^2\mathbf{b}_3 d^2\mathbf{b}'_2 d^2\mathbf{b}'_3 d^2\mathbf{b}_q$	$\frac{1}{(2\pi)^4}K_0(\sqrt{t_A}|\mathbf{b}_3+\mathbf{b}'_2|)K_0(\sqrt{t_B}|\mathbf{b}_2+\mathbf{b}'_3|)K_0(\sqrt{t_C}|\mathbf{b}'_2|)K_0(\sqrt{t_D}|\mathbf{b}_2|)$
B_{b3}	$d^2\mathbf{b}_2 d^2\mathbf{b}'_3 d^2\mathbf{b}_q$	$K_0(\sqrt{t_A}|\mathbf{b}_2+\mathbf{b}'_3+\mathbf{b}_q|)h_2(\mathbf{b}'_3,\mathbf{b}_2,t_B,t_C,t_D)$
B_{b4}	$d^2\mathbf{b}_2 d^2\mathbf{b}'_3 d^2\mathbf{b}_q$	$K_0(\sqrt{t_B}|\mathbf{b}_2+\mathbf{b}'_3|)h_2(\mathbf{b}'_3+\mathbf{b}_q,\mathbf{b}_2,t_A,t_C,t_D)$
B_{b5}	$d^2\mathbf{b}_2 d^2\mathbf{b}_3 d^2\mathbf{b}'_3 d^2\mathbf{b}_q$	$\frac{1}{(2\pi)^4}K_0(\sqrt{t_A}|\mathbf{b}'_3+\mathbf{b}_q|)K_0(\sqrt{t_B}|\mathbf{b}_2-\mathbf{b}_3-\mathbf{b}_q|)K_0(\sqrt{t_C}|\mathbf{b}_3-\mathbf{b}'_3+\mathbf{b}_q|)K_0(\sqrt{t_D}|\mathbf{b}_2|)$
B_{b6}	$d^2\mathbf{b}_2 d^2\mathbf{b}_3 d^2\mathbf{b}'_3 d^2\mathbf{b}_q$	$\frac{1}{(2\pi)^4}K_0(\sqrt{t_A}|\mathbf{b}_3+\mathbf{b}'_3|)K_0(\sqrt{t_B}|\mathbf{b}_2-\mathbf{b}_3-\mathbf{b}_q|)K_0(\sqrt{t_C}|\mathbf{b}_3+\mathbf{b}'_3+\mathbf{b}_q|)K_0(\sqrt{t_D}|\mathbf{b}_2|)$
B_{b7}	$d^2\mathbf{b}_2 d^2\mathbf{b}_3 d^2\mathbf{b}'_3 d^2\mathbf{b}_q$	$\frac{1}{(2\pi)^4}K_0(\sqrt{t_A}|\mathbf{b}_q|)K_0(\sqrt{t_B}|\mathbf{b}_2+\mathbf{b}'_3|)K_0(\sqrt{t_C}|\mathbf{b}_3+\mathbf{b}'_3-\mathbf{b}_q|)K_0(\sqrt{t_D}|\mathbf{b}_2|)$
B_{c1}	$d^2\mathbf{b}_2 d^2\mathbf{b}_3 d^2\mathbf{b}'_3$	$K_0(\sqrt{t_A}|\mathbf{b}_3|)h_2(\mathbf{b}_2-\mathbf{b}'_3,\mathbf{b}_2,t_B,t_C,t_D)$
B_{c2}	$d^2\mathbf{b}_2 d^2\mathbf{b}_3 d^2\mathbf{b}'_3$	$K_0(\sqrt{t_B}|\mathbf{b}_2-\mathbf{b}'_3|)h_2(\mathbf{b}_2-\mathbf{b}_3,\mathbf{b}_2,t_A,t_C,t_D)$
B_{c3}	$d^2\mathbf{b}_2 d^2\mathbf{b}_3 d^2\mathbf{b}'_2 d^2\mathbf{b}_q$	$\frac{1}{(2\pi)^4}K_0(\sqrt{t_A}|\mathbf{b}_2-\mathbf{b}_3-\mathbf{b}'_2|)K_0(\sqrt{t_B}|\mathbf{b}_3+\mathbf{b}_q|)K_0(\sqrt{t_C}|\mathbf{b}'_2|)K_0(\sqrt{t_D}|\mathbf{b}_2|)$
B_{c4}	$d^2\mathbf{b}_2 d^2\mathbf{b}_3 d^2\mathbf{b}'_3 d^2\mathbf{b}_q$	$\frac{1}{(2\pi)^4}K_0(\sqrt{t_A}|\mathbf{b}_2-\mathbf{b}_3|)K_0(\sqrt{t_B}|\mathbf{b}_3+\mathbf{b}_q|)K_0(\sqrt{t_C}|\mathbf{b}_2-\mathbf{b}_3-\mathbf{b}'_3-\mathbf{b}_q|)K_0(\sqrt{t_D}|\mathbf{b}_3+\mathbf{b}'_3+\mathbf{b}_q|)$
B_{c5}	$d^2\mathbf{b}_2 d^2\mathbf{b}_3 d^2\mathbf{b}'_3 d^2\mathbf{b}_q$	$\frac{1}{(2\pi)^4}K_0(\sqrt{t_A}|\mathbf{b}'_3+\mathbf{b}_q|)K_0(\sqrt{t_B}|\mathbf{b}_3+\mathbf{b}_q|)K_0(\sqrt{t_C}|\mathbf{b}_2-\mathbf{b}_3-\mathbf{b}'_3-\mathbf{b}_q|)K_0(\sqrt{t_D}|\mathbf{b}_2|)$
B_{c6}	$d^2\mathbf{b}_2 d^2\mathbf{b}_3 d^2\mathbf{b}'_3 d^2\mathbf{b}_q$	$\frac{1}{(2\pi)^4}K_0(\sqrt{t_A}|\mathbf{b}_2-\mathbf{b}_3-\mathbf{b}'_3|)K_0(\sqrt{t_B}|\mathbf{b}_3+\mathbf{b}_q|)K_0(\sqrt{t_C}|\mathbf{b}_2-\mathbf{b}_3+\mathbf{b}'_3+\mathbf{b}_q|)K_0(\sqrt{t_D}|\mathbf{b}_2|)$
B_{c7}	$d^2\mathbf{b}_2 d^2\mathbf{b}_3 d^2\mathbf{b}'_3 d^2\mathbf{b}_q$	$\frac{1}{(2\pi)^4}K_0(\sqrt{t_A}|\mathbf{b}_2+\mathbf{b}_q|)K_0(\sqrt{t_B}|\mathbf{b}_2+\mathbf{b}'_3|)K_0(\sqrt{t_C}|\mathbf{b}_2-\mathbf{b}_3-\mathbf{b}'_3-\mathbf{b}_q|)K_0(\sqrt{t_D}|\mathbf{b}_2|)$
B_{d1}	$d^2\mathbf{b}_3 d^2\mathbf{b}'_2 d^2\mathbf{b}'_3 d^2\mathbf{b}_q$	$\frac{1}{(2\pi)^4}K_0(\sqrt{t_A}|\mathbf{b}_3|)K_0(\sqrt{t_B}|\mathbf{b}'_2-\mathbf{b}'_3|)K_0(\sqrt{t_C}|\mathbf{b}_2|)K_0(\sqrt{t_D}|\mathbf{b}_2|)$
B_{d2}	$d^2\mathbf{b}_3 d^2\mathbf{b}'_2 d^2\mathbf{b}'_3$	$K_0(\sqrt{t_B}|\mathbf{b}'_2-\mathbf{b}'_3|)h_2(\mathbf{b}_3+\mathbf{b}'_2,\mathbf{b}'_2,t_A,t_C,t_D)$
B_{d3}	$d^2\mathbf{b}_3 d^2\mathbf{b}'_2 d^2\mathbf{b}'_3$	$K_0(\sqrt{t_A}|\mathbf{b}_3+\mathbf{b}'_2|)h_2(\mathbf{b}'_3,\mathbf{b}'_2,t_B,t_C,t_D)$
B_{d4}	$d^2\mathbf{b}_2 d^2\mathbf{b}_3 d^2\mathbf{b}'_2 d^2\mathbf{b}'_3$	$\frac{1}{(2\pi)^4}K_0(\sqrt{t_A}|\mathbf{b}_2-\mathbf{b}_3|)K_0(\sqrt{t_B}|\mathbf{b}'_2-\mathbf{b}'_3|)K_0(\sqrt{t_C}|\mathbf{b}_2|)K_0(\sqrt{t_D}|\mathbf{b}'_2|)$
B_{d5}	$d^2\mathbf{b}_3 d^2\mathbf{b}'_2 d^2\mathbf{b}'_3 d^2\mathbf{b}_q$	$\frac{1}{(2\pi)^4}K_0(\sqrt{t_A}|\mathbf{b}'_3+\mathbf{b}_q|)K_0(\sqrt{t_B}|\mathbf{b}'_2-\mathbf{b}'_3|)K_0(\sqrt{t_C}|\mathbf{b}_3+\mathbf{b}'_3+\mathbf{b}_q|)K_0(\sqrt{t_D}|\mathbf{b}_3-\mathbf{b}'_2+\mathbf{b}'_3+\mathbf{b}_q|)$
B_{d6}	$d^2\mathbf{b}_3 d^2\mathbf{b}'_2 d^2\mathbf{b}'_3 d^2\mathbf{b}_q$	$\frac{1}{(2\pi)^4}K_0(\sqrt{t_A}|\mathbf{b}_3+\mathbf{b}'_3|)K_0(\sqrt{t_B}|\mathbf{b}_3+\mathbf{b}'_2+\mathbf{b}_q|)K_0(\sqrt{t_C}|\mathbf{b}_3+\mathbf{b}'_3+\mathbf{b}_q|)K_0(\sqrt{t_D}|\mathbf{b}'_2|)$
B_{d7}	$d^2\mathbf{b}_3 d^2\mathbf{b}'_2 d^2\mathbf{b}'_3 d^2\mathbf{b}_q$	$\frac{1}{(2\pi)^4}K_0(\sqrt{t_A}|\mathbf{b}_q|)K_0(\sqrt{t_B}|\mathbf{b}'_2-\mathbf{b}'_3|)K_0(\sqrt{t_C}|\mathbf{b}_3+\mathbf{b}'_3+\mathbf{b}_q|)K_0(\sqrt{t_D}|\mathbf{b}'_2|)$
B_{e1}	$d^2\mathbf{b}_2 d^2\mathbf{b}_3 d^2\mathbf{b}'_3 d^2\mathbf{b}_q$	$\frac{1}{(2\pi)^4}K_0(\sqrt{t_A}|\mathbf{b}_q|)K_0(\sqrt{t_B}|\mathbf{b}_3|)K_0(\sqrt{t_C}|\mathbf{b}_2-\mathbf{b}_3-\mathbf{b}'_3-\mathbf{b}_q|)K_0(\sqrt{t_D}|\mathbf{b}_2|)$
B_{e2}	$d^2\mathbf{b}_3 d^2\mathbf{b}'_2 d^2\mathbf{b}'_3 d^2\mathbf{b}_q$	$\frac{1}{(2\pi)^4}K_0(\sqrt{t_A}|\mathbf{b}_q|)K_0(\sqrt{t_B}|\mathbf{b}_3+\mathbf{b}'_2|)K_0(\sqrt{t_C}|\mathbf{b}_3+\mathbf{b}'_3+\mathbf{b}_q|)K_0(\sqrt{t_D}|\mathbf{b}'_2|)$
B_{e3}	$d^2\mathbf{b}_2 d^2\mathbf{b}_3 d^2\mathbf{b}'_3 d^2\mathbf{b}_q$	$\frac{1}{(2\pi)^4}K_0(\sqrt{t_A}|\mathbf{b}_q|)K_0(\sqrt{t_B}|\mathbf{b}_2-\mathbf{b}_3|)K_0(\sqrt{t_C}|\mathbf{b}_3+\mathbf{b}'_3+\mathbf{b}_q|)K_0(\sqrt{t_D}|\mathbf{b}_2|)$
B_{e4}	$d^2\mathbf{b}_3 d^2\mathbf{b}'_2 d^2\mathbf{b}'_3 d^2\mathbf{b}_q$	$\frac{1}{(2\pi)^4}K_0(\sqrt{t_A}|\mathbf{b}_q|)K_0(\sqrt{t_B}|\mathbf{b}_3-\mathbf{b}'_2|)K_0(\sqrt{t_C}|\mathbf{b}_3-\mathbf{b}'_2+\mathbf{b}'_3+\mathbf{b}_q|)K_0(\sqrt{t_D}|\mathbf{b}'_2|)$
B_{f1}	$d^2\mathbf{b}_2 d^2\mathbf{b}_3 d^2\mathbf{b}'_3 d^2\mathbf{b}_q$	$\frac{1}{(2\pi)^4}K_0(\sqrt{t_A}|\mathbf{b}_2-\mathbf{b}_3-\mathbf{b}'_3|)K_0(\sqrt{t_B}|\mathbf{b}_2-\mathbf{b}'_3-\mathbf{b}_q|)K_0(\sqrt{t_C}|\mathbf{b}_2-\mathbf{b}_3-\mathbf{b}'_3-\mathbf{b}_q|)K_0(\sqrt{t_D}|\mathbf{b}_2|)$
B_{f2}	$d^2\mathbf{b}_3 d^2\mathbf{b}'_2 d^2\mathbf{b}'_3 d^2\mathbf{b}_q$	$\frac{1}{(2\pi)^4}K_0(\sqrt{t_A}|\mathbf{b}_3+\mathbf{b}'_3|)K_0(\sqrt{t_B}|\mathbf{b}'_2-\mathbf{b}'_3-\mathbf{b}_q|)K_0(\sqrt{t_C}|\mathbf{b}_3+\mathbf{b}'_3+\mathbf{b}_q|)K_0(\sqrt{t_D}|\mathbf{b}'_2|)$
B_{f3}	$d^2\mathbf{b}_2 d^2\mathbf{b}_3 d^2\mathbf{b}'_3 d^2\mathbf{b}_q$	$\frac{1}{(2\pi)^4}K_0(\sqrt{t_A}|\mathbf{b}_3+\mathbf{b}'_3|)K_0(\sqrt{t_B}|\mathbf{b}_2+\mathbf{b}'_3+\mathbf{b}_q|)K_0(\sqrt{t_C}|\mathbf{b}_3+\mathbf{b}'_3+\mathbf{b}_q|)K_0(\sqrt{t_D}|\mathbf{b}_2|)$
B_{f4}	$d^2\mathbf{b}_3 d^2\mathbf{b}'_2 d^2\mathbf{b}'_3 d^2\mathbf{b}_q$	$\frac{1}{(2\pi)^4}K_0(\sqrt{t_A}|\mathbf{b}'_2-\mathbf{b}_3-\mathbf{b}'_3|)K_0(\sqrt{t_B}|\mathbf{b}'_3+\mathbf{b}_q|)K_0(\sqrt{t_C}|\mathbf{b}_3-\mathbf{b}'_2+\mathbf{b}'_3+\mathbf{b}_q|)K_0(\sqrt{t_D}|\mathbf{b}'_2|)$
B_{g1}	$d^2\mathbf{b}_2 d^2\mathbf{b}'_3 d^2\mathbf{b}_q$	$K_0(\sqrt{t_D}|\mathbf{b}_2|)h_2(\mathbf{b}_2+\mathbf{b}'_3+\mathbf{b}_q,\mathbf{b}_2-\mathbf{b}'_3,t_A,t_B,t_C)$
B_{g2}	$d^2\mathbf{b}_2 d^2\mathbf{b}'_3 d^2\mathbf{b}_q$	$K_0(\sqrt{t_D}|\mathbf{b}'_2|)h_2(\mathbf{b}'_3+\mathbf{b}_q,\mathbf{b}'_3,t_A,t_B,t_C)$
B_{g3}	$d^2\mathbf{b}_2 d^2\mathbf{b}_3 d^2\mathbf{b}_q$	$K_0(\sqrt{t_D}|\mathbf{b}_2|)h_2(\mathbf{b}_3,\mathbf{b}_3+\mathbf{b}_q,t_A,t_B,t_C)$
B_{g4}	$d^2\mathbf{b}'_2 d^2\mathbf{b}'_3 d^2\mathbf{b}_q$	$K_0(\sqrt{t_D}|\mathbf{b}'_2|)h_2(\mathbf{b}'_2-\mathbf{b}'_3-\mathbf{b}_q,\mathbf{b}'_2-\mathbf{b}'_3,t_A,t_B,t_C)$

$$b_1^{(')} = \left| b_2^{(')} - b_3^{(')} \right|, \qquad \text{(A3)}$$

and the other $b_l^{(')}$ defined by permutation. Here, we only present the results of $[\mathcal{D}b]_{R_{ij}}$, $\Omega_{R_{ij}}$, and $t_{A,B,C,D}$ for the C, B,

and E_q diagrams. The remaining results are the same as those for $\Lambda_b \to \Lambda\phi$ and can be found in [60].

In Table VII, we give the expressions of $H^\sigma_{R_{ij}}$ for a representative set of diagrams for each type, as shown in Fig. 1, while those for others can be derived in an analogous way.

TABLE VI. Virtualities of the internal gluon $t_{A,B}$ and quark $t_{C,D}$ for the C, B, and E_q diagrams.

R_{ij}	$\frac{t_A}{M^2}$	$\frac{t_B}{M^2}$	$\frac{t_C}{M^2}$	$\frac{t_D}{M^2}$	R_{ij}	$\frac{t_A}{M^2}$	$\frac{t_B}{M^2}$	$\frac{t_C}{M^2}$	$\frac{t_D}{M^2}$
C_{a1}	$x_2 y$	$y(1-x_1)$	$y(1-x_1-x_3')$	$y+x_3'(1-y)$	Eq_{a1}	$x_3 x_3'$	$x_2'(y-1)$	$x_3'(1-x_1)$	$(y-1)(1-x_3')$
C_{a2}	$x_2 y$	$y(x_2-x_3')$	$y(1-x_1-x_3')$	$y+x_3'(1-y)$	Eq_{a2}	$x_3 x_3'$	$x_2'(y-1)$	x_3+y-1	$(y-1)(1-x_3')$
C_{a3}	$x_2 y$	$x_3 x_3'$	x_3+y	$y+x_3'(1-y)$	Eq_{a3}	$x_3 x_3'$	$x_2'(y-1)$	$x_3(1-x_2')$	x_3+y-1
C_{a4}	$x_2 y$	$x_3 x_3'$	x_2+x_3'	$y+x_3'(1-y)$	Eq_{a4}	$x_3 x_3'$	$x_2'(y-1)$	$x_2+x_3'(1-x_2)$	$(y-1)(1-x_3')$
C_{a5}	$x_2 y$	$x_3 x_3'$	$y(x_2-x_2')$	x_2+x_3'	Eq_{a5}	$x_3 x_3'$	$x_2'(y-1)$	$x_3'(x_3-y)$	$(y-1)(1-x_3')$
C_{a6}	$x_2 y$	$x_3 x_3'$	$y(x_2-x_1')$	x_2+x_3'	Eq_{a6}	$x_3 x_3'$	$x_2'(y-1)$	$x_3(1-x_1')$	x_3+y-1
C_{a7}	$x_2 y$	$x_3 x_3'$	x_2	x_2+x_3'	Eq_{a7}	$x_3 x_3'$	$x_2'(y-1)$	$x_3'(1-x_1)$	x_3+y-1
C_{b1}	$x_2 y$	$y(1-x_1-x_3')$	$y(1-x_1)$	$y(x_1+x_1')$	Eq_{b1}	$x_3 x_3'$	$(1-x_1')(x_3+y-1)$	$(y-x_1)(1-x_1')$	$(1-x_1')(y-x_1)$
C_{b2}	$x_2 y$	$y(1-x_1-x_3')$	$y(x_2-x_3')$	$y(x_1+x_1')$	Eq_{b2}	$x_3 x_3'$	$(1-x_1')(x_3+y-1)$	$x_3(1-x_2')$	$x_2'(x_2+y-1)$
C_{b3}	$x_2 y$	$x_3 x_3' y$	x_3+y	$x_3(1-x_1')$	Eq_{b3}	$x_3 x_3'$	$x_2'(y-1)$	$x_2+x_3'(1-x_2)$	$x_2'(x_2+y-1)$
C_{b4}	$x_2 y$	$x_3 x_3'$	$(y-x_3)(x_2-x_2'-x_3')$	$x_3(1-x_1')$	Eq_{b4}	$x_3 x_3'$	$x_2'(y-1)$	$x_3'(x_3-y)$	$x_2'(x_2+y-1)$
C_{b5}	$x_2 y$	$x_3 x_3'$	$y(x_2-x_2')$	$x_2-x_2'-x_3'(y-x_3)$	Eq_{b5}	$x_3 x_3'$	$x_2'(y-1)$	$x_3(1-x_1')$	$x_2'(x_2+y-1)$
C_{b6}	$x_2 y$	$x_3 x_3'$	$y(x_2-x_1')$	$x_3(1-x_1')$	Eq_{b6}	$x_3 x_3'$	$(1-x_1')(x_3+y-1)$	$x_3'(1-x_1)$	$(1-x_1')(y-x_1)$
C_{b7}	$x_2 y$	$x_3 x_3'$	x_2	$x_3(1-x_1')$	Eq_{b7}	$x_3 x_3'$	$(1-x_1')(x_3+y-1)$	$x_3(1-x_1')$	$(1-x_1')(y-x_1)$
C_{c1}	$x_2 y$	$y(1-x_1)$	$y(1-x_1-x_3')$	$y(x_2'-x_1)$	Eq_{c1}	$x_3 x_3'$	$x_2'(y-1)$	$x_3'(1-x_1)$	$(y-1)(x_2+1)-x_2'$
C_{c2}	$x_2 y$	$y(x_2-x_3')$	$y(1-x_1-x_3')$	$y(x_2'-x_1)$	Eq_{c2}	$x_3 x_3'$	$x_2'(y-1)$	$x_3(1-x_2')$	$(y-1)(x_2+1)-x_2'$
C_{c3}	$x_2 y$	$x_3 x_3'$	x_3+y	$x_3(1-x_2')$	Eq_{c3}	$x_3 x_3'$	$x_2'(y-1)$	$x_2+x_3'(1-x_2)$	$x_1(x_2-y)+1$
C_{c4}	$x_2 y$	$x_3 x_3'$	$y(x_2-x_2')$	$x_3(1-x_2')$	Eq_{c4}	$x_3 x_3'$	$x_2'(y-1)$	$x_1'(x_2-y)+1$	$(1-x_2')(1-x_1-y)+1$
C_{c5}	$x_2 y$	$x_3 x_3'$	$(x_3-y)(1-x_2-x_2'-x_2')$	$x_3(1-x_2')$	Eq_{c5}	$x_3 x_3'$	$x_2'(y-1)$	$x_3'(x_3+y+1)$	$(1-x_2')(1-x_1-y)+1$
C_{c6}	$x_2 y$	$x_3 x_3'$	$y(x_2-x_1')$	$(y-x_3)(x_2+x_2'-1)$	Eq_{c6}	$x_3 x_3'$	$(1-x_1')(x_3+y-1)$	$x_3(1-x_1')$	$x_1'(x_2-y)+1$
C_{c7}	$x_2 y$	$x_3 x_3'$	x_2	$x_3(1-x_2')$	Eq_{c7}	$x_3 x_3'$	$(1-x_1')(x_3+y-1)$	$x_3'(1-x_1)$	$x_1'(x_2-y)+1$
C_{d1}	$x_2 y$	$y(1-x_1-x_3')$	$y(1-x_1)$	$1-x_1-x_3$	Eq_{d1}	$x_3 x_3'$	$(1-x_1')(x_3+y-1)$	$x_3(1-x_2')$	$-x_2'$
C_{d2}	$x_2 y$	$y(1-x_1-x_3')$	$y(x_2-x_3')$	$1-x_1-x_3$	Eq_{d2}	$x_3 x_3'$	$x_2'(y-1)$	$x_3(1-x_2')$	$-x_2'$
C_{d3}	$x_2 y$	$x_3 x_3'$	x_3+y	$x_3'(x_3+y-1)$	Eq_{d3}	$x_3 x_3'$	$x_2'(y-1)$	$x_2+x_3'(1-x_2)$	$-x_2'$
C_{d4}	$x_2 y$	$x_3 x_3'$	$y(x_2-x_2')$	$x_3'(x_3+y-1)$	Eq_{d4}	$x_3 x_3'$	$x_2'(y-1)$	$(x_3-1)(1-x_1')$	$-x_2'$
C_{d5}	$x_2 y$	$x_3 x_3'$	$y(x_2-x_1')$	$x_3'(x_3+y-1)$	Eq_{d5}	$x_3 x_3'$	$x_2'(y-1)$	$x_3'(x_3-y)$	$(1-x_1')(x_3-1)$
C_{d6}	$x_2 y$	$x_3 x_3'$	x_2	$(1-x_1')(x_3-1)$	Eq_{d6}	$x_3 x_3'$	$(1-x_1')(x_3+y-1)$	$x_3'(x_3+y+1)$	$(1-x_1')(x_3-1)$
C_{d7}	$x_2 y$	$x_3 x_3'$	$y(x_2-x_1')$	$x_3'(x_3+y-1)$	Eq_{d7}	$x_3 x_3'$	$(1-x_1')(x_3+y-1)$	$x_3(1-x_1')$	$(x_2-x_3')(1-x_3)$
C_{e1}	$x_3 x_3'$	$x_3'(1-x_1-y)$	$x_3'(1-x_1)$	$y+x_3'(1-y)$	Eq_{e1}	$x_2'(y-1)$	$(1-x_1')(x_3+y-1)$	$(y-1)(1-x_1')$	$(1-x_1')(y-x_1)$
C_{e2}	$x_3 x_3'$	$x_3'(1-x_1-y)$	$x_3'(1-x_1)$	$(1-x_1')(1-x_1-y)$	Eq_{e2}	$x_2'(y-1)$	$(1-x_1')(x_3+y-1)$	$(y-1)(1-x_1)$	x_3+y-1
C_{e3}	$x_3 x_3'$	$x_3'(1-x_1-y)$	$x_3'(1-x_1)$	$(1-x_2')(1-x_1-y)$	Eq_{e3}	$x_2'(y-1)$	$(1-x_1')(x_3+y-1)$	$(y-1)(1-x_1)$	$x_1'(x_2-y)+1$
C_{e4}	$x_3 x_3'$	$x_3'(1-x_1-y)$	$x_3'(1-x_1)$	$-x_1 x_3'$	Eq_{e4}	$x_2'(y-1)$	$(1-x_1')(x_3+y-1)$	$(y-1)(1-x_1)$	$(x_3-1)(1-x_1')$

(Table continued)

TABLE VI. (Continued)

R_{ij}	$\frac{t_A}{M^2}$	$\frac{t_B}{M^2}$	$\frac{t_C}{M^2}$	$\frac{t_D}{M^2}$	R_{ij}	$\frac{t_A}{M^2}$	$\frac{t_B}{M^2}$	$\frac{t_C}{M^2}$	$\frac{t_D}{M^2}$
C_{f1}	$x_3 x_3'$	$x_3'(1-x_1-y)$	$x_3'(x_3-y)$	$y+x_3'(1-y)$	Eq_{f1}	$x_2'(y-1)$	$(1-x_1')(x_3+y-1)$	$x_2'(x_3+y-1)$	$(1-x_1')(y-x_1)$
C_{f2}	$x_3 x_3'$	$x_3'(1-x_1-y)$	$x_3'(x_3-y)$	$(1-x_1')(1-x_1-y)$	Eq_{f2}	$x_2'(y-1)$	$(1-x_1')(x_3+y-1)$	$x_2'(x_3+y-1)$	x_3+y-1
C_{f3}	$x_3 x_3'$	$x_3'(1-x_1-y)$	$x_3'(x_3-y)$	$(1-x_2')(1-x_1-y)$	Eq_{f3}	$x_2'(y-1)$	$(1-x_1')(x_3+y-1)$	$x_2'(x_3+y-1)$	$x_1'(x_2-y)+1$
C_{f4}	$x_3 x_3'$	$x_3'(1-x_1-y)$	$x_3'(x_3-y)$	$-x_1 x_3'$	Eq_{f4}	$x_2'(y-1)$	$(1-x_1')(x_3+y-1)$	$x_2'(x_3+y-1)$	$(1-x_1')(x_3-1)$
C_{g2}	x_2	$x_3 x_3'$	$(x_3-y)(x_3'-x_2)$	$x_2-x_2'-x_3'(y-x_3)$	Eq_{g1}	$x_2'(y-1)$	$x_3 x_3'$	$(1-x_1')(x_3+y-1)$	$(1-x_1')(y-x_1)$
C_{g3}	x_2	$x_3 x_3'$	$(x_3-y)(x_3'-x_2)$	$(x_2-x_3')(1-x_3)$	Eq_{g3}	$x_2'(y-1)$	$x_3 x_3'$	$(1-x_1')(x_3+y-1)$	$x_1'(x_2-y)+1$
C_{g4}	x_2	$x_3 x_3'$	$(x_3-y)(x_3'-x_2)$	$(y-x_3)(x_2+x_2'-1)$	Eq_{g4}	$x_2'(y-1)$	$x_3 x_3'$	$(1-x_1')(x_3+y-1)$	$(x_3-1)(1-x_1')$
B_{a1}	$x_3 y$	$x_3'(y-1)$	$x_2+y(1-x_2)$	$(1-x_2')(y-1)$	B_{a2}	$x_3 y$	$x_3'(y-1)$	$y(x_3-x_2')$	$(1-x_2')(y-1)$
B_{a3}	$x_3 y$	$x_3'(y-1)$	$y(1-x_1)$	$(1-x_2')(y-1)$	B_{a4}	$x_3 y$	$x_3'(y-1)$	$x_3+x_2'-1$	$(1-x_2')(y-1)$
B_{a5}	$x_3 y$	$x_3'(y-1)$	$y(x_3-x_1')$	$x_3+x_2'-1$	B_{a6}	$x_3 y$	$x_3'(y-1)$	$y(x_3-x_3')$	$x_3+x_2'-1$
B_{a7}	$x_3 y$	$x_3'(y-1)$	x_3	$x_3+x_2'-1$	B_{b1}	$x_3 y$	$x_3'(y-1)$	$x_2+y(1-x_2)$	$(1-y)(x_2-x_3')$
B_{b2}	$x_3 y$	$x_3'(y-1)$	$y(x_3-x_2')$	$(1-y)(x_2-x_3')$	B_{b3}	$x_3 y$	$x_3'(y-1)$	$y(1-x_1)$	$1-x_1-x_3'$
B_{b4}	$x_3 y$	$x_3'(y-1)$	$x_2+x_3-x_3'$	$(1-y)(x_2-x_3')$	B_{b5}	$x_3 y$	$x_3'(y-1)$	$y(x_3-x_1')$	$(1-y)(x_2-x_3')$
B_{b6}	$x_3 y$	$x_3'(y-1)$	$y(x_3-x_3')$	$1-x_1-x_3'$	B_{b7}	$x_3 y$	$x_3'(y-1)$	x_3	$1-x_1-x_3'$
B_{c1}	$x_3 y$	$x_3'(y-1)$	$x_2+y(1-x_2)$	1	B_{c2}	$x_3 y$	$x_3'(y-1)$	1	$1-y(1-x_2')$
B_{c3}	$x_3 y$	$x_3'(y-1)$	$y(x_3-x_2')$	$1-y(1-x_2')$	B_{c4}	$x_3 y$	$x_3'(y-1)$	$y(1-x_1)$	$1-y(1-x_2')$
B_{c5}	$x_3 y$	$x_3'(y-1)$	$y(x_3-x_1')$	$1-y(1-x_2')$	B_{c6}	$x_3 y$	$x_3'(y-1)$	$y(x_3-x_3')$	1
B_{c7}	$x_3 y$	x_3-x_3'	x_3	1	B_{d1}	$x_3 y$	x_3-x_3'	$x_2+y(1-x_2)$	$(y-1)(1-x_1')$
B_{d2}	$x_3 y$	$x_3'(y-1)$	$x_3-x_2'-x_3'$	$(y-1)(1-x_1')$	B_{d3}	$x_3 y$	$x_3'(y-1)$	$y(x_3-x_2')$	$x_3+x_1'-1$
B_{d4}	$x_3 y$	$x_3'(y-1)$	$y(1-x_1)$	$(y-1)(1-x_1')$	B_{d5}	$x_3 y$	$x_3'(y-1)$	$y(x_3-x_1')$	$(y-1)(1-x_1')$
B_{d6}	$x_3 y$	x_3-x_3'	$y(x_3-x_3')$	$x_3+x_1'-1$	B_{d7}	$x_3 y$	x_3-x_3'	x_3	$x_3+x_1'-1$
B_{e1}	$x_3'(y-1)$	x_3-x_3'	$-x_3'$	1	B_{e2}	$x_3'(y-1)$	x_3-x_3'	$-x_3'$	$x_3+x_1'-1$
B_{e3}	$x_3'(y-1)$	x_3-x_3'	$-x_3'$	$1-x_1-x_3'$	B_{e4}	$x_3'(y-1)$	x_3-x_3'	$-x_3'$	$x_3+x_1'-1$
B_{f1}	$x_3'(y-1)$	x_3-x_3'	$(1-y)(x_3-x_3')$	$1-x_1-x_3'$	B_{f2}	$x_3'(y-1)$	x_3-x_3'	$(1-y)(x_3-x_3')$	$x_3+x_1'-1$
B_{f3}	$x_3'(y-1)$	x_3-x_3'	$(1-y)(x_3-x_3')$	$1-x_1-x_3'$	B_{f4}	$x_3'(y-1)$	x_3-x_3'	$(1-y)(x_3-x_3')$	$x_3+x_1'-1$
B_{g1}	$x_3 y$	$x_3'(y-1)$	x_3-x_3'	1	B_{g2}	$x_3 y$	$x_3'(y-1)$	x_3-x_3'	$x_3+x_1'-1$
B_{g3}	$x_3 y$	$x_3'(y-1)$	x_3-x_3'	1	B_{g4}	$x_3 y$	$x_3'(y-1)$	x_3-x_3'	$x_3+x_1'-1$

TABLE VII. Expressions of $H_{R_{li}}^\sigma$ for the six representative diagrams in Fig 1. The ratios $r_0^{q,s}$ are defined by $r_0^{q,s}=m_0^{q,s}/M$.

	$\dfrac{M_S}{16M^4}$	$\dfrac{M_P}{16M^4}$
$H_{T_{c7}}^{LL}$	$2\phi_q^A(x_3'x_3(\Psi_3^{+-}-(r_\Lambda-1)\Phi^T(x_2-y)-\Psi_4x_2'x_2'r_\Lambda(\Phi^A-\Phi^V))$ $-2\Psi_2\Phi^A(r_\Lambda-1)(y-x_2)(x_3+y-1)-\Psi_3^{-+}x_2'r_\Lambda\Phi^T(x_3+y-1))$	$2\phi_q^A((r_\Lambda-1)(x_3+y-1)(2\Psi_2\Phi^A(y-x_2)+\Psi_3^{+-}x_2'\Phi^T)$ $+x_3'r_\Lambda(\Psi_4x_2'x_2'(\Phi^A+\Phi^V)+\Psi_3^{+-}\Phi^T(y-x_2)))$
$H_{T_{c7}}^{SP}$	$2\phi_q^A(x_3'x_3r_\Lambda(\Psi_4x_3(\Phi^A-\Phi^V)-\Psi_3^{-+}\Phi^T(x_3+y-1))$ $+(r_\Lambda+1)(y-x_2)(2\Psi_2\Phi^A(x_3+y-1)-x_3'\Psi_3^{+-}\Phi^T))$	$2\phi_q^A(x_3'x_3r_\Lambda(\Psi_3^{+-}\Phi^T(y-x_2)-\Psi_4x_2'(\Phi^A+\Phi^V))$ $-(r_\Lambda+1)(x_3+y-1)(2\Psi_2\Phi^A(y-x_2)-\Psi_3^{-+}x_2'\Phi^T))$
$H_{C_{d7}}^{LL}$	$r_\Lambda(3(x_3-1)\Phi^T(x_2\Psi_3^{+-}\phi_q^A+4r_0^q(\Psi_2-x_2\Psi_4)\phi_q^P)$ $+2(x_3'-x_2)\Psi_3^{+-}r_0^q(\Phi^A-\Phi^V)\phi_q^P)$	$r_\Lambda(2r_0^q\phi_q^P((x_2-x_3')\Psi_3^{+-}(\Phi^A-\Phi^V)+6(x_3-1)\Phi^T(\Psi_2-x_2\Psi_4))$ $+3x_2(x_3-1)\Psi_3^{+-}\Phi^T\phi_q^A)$
$H_{C_{d7}}^{SP}$	$2(x_2-x_3')\Psi_3^{+-}r_0^q r_\Lambda(\Phi^A+\Phi^V)\phi_q^P$ $-(x_3-1)(r_\Lambda-2)\Phi^T(x_2\Psi_3^{+-}\phi_q^A+4r_0^q(\Psi_2-x_2\Psi_4)\phi_q^P)$	$-x_2(x_3-1)\Psi_3^{+-}(r_\Lambda+2)\Phi^T\phi_q^A-2r_0^q\phi_q^P((x_2-x_3')\Psi_3^{+-}r_\Lambda(\Phi^A+\Phi^V)$ $+2(x_3-1)(r_\Lambda+2)\Phi^T(\Psi_2-x_2\Psi_4))$
$H_{Eq_{a2}}^{LL}$	$r_0^q((y-1)\Phi^A(\Psi_3^{-+}(r_\Lambda-1)(x_3+y-1)(\phi_q^P+\phi_q^T)+\Psi_3^{+-}r_\Lambda(\phi_q^P-\phi_q^T))$ $+(y-1)\Phi^V(\Psi_3^{-+}(r_\Lambda-1)(x_3+y-1)(\phi_q^P+\phi_q^T)+\Psi_3^{+-}r_\Lambda(\phi_q^P-\phi_q^T))$ $+2\Phi^T(x_3+y-1)(\phi_q^P+\phi_q^T)(2\Psi_2(y-1)(r_\Lambda-1)-\Psi_4(x_3'-1)r_\Lambda))$	$r_0^q(-(y-1)\Phi^A(\Psi_3^{-+}(r_\Lambda+1)(x_3+y-1)(\phi_q^P+\phi_q^T)+\Psi_3^{+-}r_\Lambda(\phi_q^P-\phi_q^T))$ $-(y-1)\Phi^V(\Psi_3^{-+}(r_\Lambda+1)(x_3+y-1)(\phi_q^P+\phi_q^T)+\Psi_3^{+-}r_\Lambda(\phi_q^P-\phi_q^T))$ $+2\Phi^T(x_3+y-1)(\phi_q^P+\phi_q^T)(2\Psi_2(y-1)(r_\Lambda+1)-\Psi_4(x_3'-1)r_\Lambda))$
$H_{Eq_{a2}}^{SP}$	$r_\Lambda\Phi^T(\phi_q^A((y-1)\Psi_3^{-+}+(x_3'-1)\Psi_3^{+-}(x_3+y-1))$ $+6(y-1)r_0^q(\Psi_2(x_3+y-1)-\Psi_4)(\phi_q^P-\phi_q^T))$ $+\Phi^V((x_3'-1)\Psi_3^{+-}r_0^q r_\Lambda(x_3+y-1)(\phi_q^P+\phi_q^T)$ $-2(y-1)(r_\Lambda-1)\phi_q^A r_\Lambda(\Psi_2(x_3+y-1)-\Psi_4))$ $+\Phi^A(2(1-y)(r_\Lambda-1)\phi_q^A(\Psi_2(x_3+y-1)-\Psi_4)$ $-(x_3'-1)\Psi_3^{+-}r_0^q r_\Lambda(x_3+y-1)(\phi_q^P+\phi_q^T)))$	$\phi_q^A(2\Psi_2(y-1)(r_\Lambda+1)(x_3+y-1)(\Phi^A+\Phi^V)-2\Psi_4(y-1)(r_\Lambda+1)(\Phi^A+\Phi^V)$ $+r_\Lambda\Phi^T((y-1)\Psi_3^{-+}+(x_3'-1)\Psi_3^{+-}(x_3+y-1)))$ $+r_0^q r_\Lambda(\Phi^A(x_3'-1)\Psi_3^{+-}(x_3+y-1)(\phi_q^P+\phi_q^T)$ $-(x_3'-1)\Psi_3^{+-}\Phi^V(x_3+y-1)(\phi_q^P+\phi_q^T)$ $+6(y-1)\Phi^T(\Psi_2(x_3+y-1)-\Psi_4)(\phi_q^P-\phi_q^T))$
$H_{Es_{d2}}^{LL}$	$r_0^s\phi_s^P(2(x_3-1)(\Phi^A+\Phi^V)(\Psi_2(r_\Lambda-1)-\Psi_4x_1'r_\Lambda)+\Phi^T(2(x_3-1)\Psi_3^{-+}(r_\Lambda-1)$ $-(x_2'-1)\Psi_3^{+-}(r_\Lambda+r_\Lambda))-\frac{1}{2}x_1'(1-x_3)\phi_s^A(2\Psi_4(r_\Lambda-1)(\Phi^A-\Phi^V)-\Psi_3^{-+}r_\Lambda\Phi^T)$	$r_0^s\phi_s^P(2(x_3-1)(\Phi^A+\Phi^V)(\Psi_2(r_\Lambda+1)-\Psi_4x_1'r_\Lambda)+\Phi^T((x_2'-1)\Psi_3^{+-}-\Psi_3^{-+}r_\Lambda$ $-2(x_3-1)\Psi_3^{-+}(r_\Lambda+1)))+\frac{1}{2}x_1'(1-x_3)\phi_s^A(2\Psi_4(r_\Lambda+1)(\Phi^A-\Phi^V)$ $+\Psi_3^{-+}r_\Lambda\Phi^T)$
$H_{Es_{d2}}^{SP}$	$r_0^s\phi_s^P(2(r_\Lambda-1)(\Phi^A-\Phi^V)(\Psi_4(x_2'-1)+(x_3-1)\Psi_2)-r_\Lambda\Phi^T(2x_1'(x_3-1)\Psi_3^{+-}$ $-\Psi_3^{-+}(x_2'-1)))+\frac{1}{2}x_1'(x_3-1)\Psi_3^{+-}(r_\Lambda-2)\Phi^T\phi_s^A$	$2(r_\Lambda+1)r_0^s(\Phi^A-\Phi^V)(\Psi_4(x_2'-1)+(x_3-1)\Psi_2)\phi_s^P$ $+\frac{1}{2}x_1'(x_3-1)\Psi_3^{+-}(r_\Lambda+2)\Phi^T\phi_s^A-r_\Lambda r_0^s\Phi^T\phi_s^P(2x_1'(1-x_3)\Psi_3^{+-}-\Psi_3^{-+}(x_2'-1))$
$H_{B_{b3}}^{LL}$	$r_\Lambda(y(x_1+x_3'-1)\Phi^V(2\Psi_2\phi_q^A+r_0^q(\Psi_3^{-+}+\Psi_3^{+-})(\phi_q^P+\phi_q^T)$ $-3\Phi^T((1-x_1)\phi_q^A(\Psi_3^{-+}+\Psi_3^{+-})+2r_0^q((1-x_1)\Psi_4(\phi_q^P+\phi_q^T)$ $+\Psi_2y(\phi_q^T-\phi_q^P)))+y\Phi^A(1-x_1-x_3')(2\Psi_2\phi_q^A+r_0^q(\Psi_3^{-+}+\Psi_3^{+-})(\phi_q^P+\phi_q^T))$	$r_\Lambda(y(x_3'-x_3-x_2)(\Phi^A-\Phi^V)(2\Psi_2\phi_q^A+r_0^q(\Psi_3^{-+}+\Psi_3^{+-})(\phi_q^P+\phi_q^T)$ $-3\Phi^T((1-x_1)\phi_q^A(\Psi_3^{-+}+\Psi_3^{+-})+2r_0^q((1-x_1)\Psi_4(\phi_q^P+\phi_q^T)$ $+\Psi_2y(\phi_q^T-\phi_q^P))))$
$H_{B_{b3}}^{SP}$	$y(x_1+x_3'-1)r_\Lambda\Phi^V(2\Psi_2\phi_q^A+Mr_0^q(\Psi_3^{-+}+\Psi_3^{+-})(\phi_q^P+\phi_q^T)$ $-y\Phi^A(1-x_1-x_3')r_\Lambda(2\Psi_2\phi_q^A+Mr_0^q(\Psi_3^{-+}+\Psi_3^{+-})(\phi_q^P+\phi_q^T))$ $+(r_\Lambda-2)\Phi^T((1-x_1)\phi_q^A(\Psi_3^{-+}+\Psi_3^{+-})+2r_0^q((1-x_1)\Psi_4(\phi_q^P+\phi_q^T)$ $+\Psi_2y(\phi_q^T-\phi_q^P))))$	$y(1-x_1-x_3')r_\Lambda(\Phi^A+\Phi^V)(2\Psi_2\phi_q^A+r_0^q(\Psi_3^{-+}+\Psi_3^{+-})(\phi_q^P+\phi_q^T))$ $+(r_\Lambda+2)\Phi^T((1-x_1)\phi_q^A(\Psi_3^{-+}+\Psi_3^{+-})+2r_0^q((1-x_1)\Psi_4(\phi_q^P+\phi_q^T)$ $+\Psi_2y(\phi_q^T-\phi_q^P)))$
$H_{B'_{a3}}^{LL}$	$x_3'r_\Lambda\phi_s^A(2\Psi_4x_3'(\Phi^A-\Phi^V)+3x_1\Psi_3^{+-}\Phi^T)$	$-r_\Lambda x_3'\phi_s^A(2\Psi_4x_3'(\Phi^A-\Phi^V)-3x_1\Psi_3^{+-}\Phi^T)$
$H_{B'_{a3}}^{SP}$	$-x_3'\phi_s^A(x_1\Psi_3^{+-}(r_\Lambda-2)\Phi^T+2\Psi_4x_3'r_\Lambda(\Phi^A+\Phi^V))$	$x_3'\phi_s^A(2\Psi_4x_3'r_\Lambda(\Phi^A+\Phi^V)-x_1\Psi_3^{+-}(r_\Lambda+2)\Phi^T)$

[1] H. Leutwyler, On the $1/N$-expansion in chiral perturbation theory, Nucl. Phys. B, Proc. Suppl. **64**, 223 (1998).

[2] R. Kaiser and H. Leutwyler, Large N_c in chiral perturbation theory, Eur. Phys. J. C **17**, 623 (2000).

[3] T. Feldmann, P. Kroll, and B. Stech, Mixing and decay constants of pseudoscalar mesons, Phys. Rev. D **58**, 114006 (1998).

[4] T. Feldmann, P. Kroll, and B. Stech, Mixing and decay constants of pseudoscalar mesons: The sequel, Phys. Lett. B **449**, 339 (1999).

[5] H. Harari, Experimental consequences of a small mixture of $c\bar{c}$ in the η' and η mesons, Phys. Lett. **60B**, 172 (1976).

[6] Y. D. Tsai, H. n. Li, and Q. Zhao, η_c mixing effects on charmonium and B meson decays, Phys. Rev. D **85**, 034002 (2012).

[7] R. Escribano and J. Nadal, On the gluon content of the η and eta' mesons, J. High Energy Phys. 05 (2007) 006.

[8] V. Mathieu and V. Vento, Pseudoscalar glueball and $\eta - \eta'$ mixing, Phys. Rev. D **81**, 034004 (2010).

[9] M. R. Ahmady, E. Kou, and A. Sugamoto, Non-spectator contribution: A mechanism for inclusive $B \to X_s \eta'$ and exclusive $B \to K^{(*)}\eta'$ decays, Phys. Rev. D **58**, 014015 (1998).

[10] M. Beneke and M. Neubert, Flavor singlet B-decay amplitudes in QCD factorization, Nucl. Phys. **B651**, 225 (2003).

[11] F. Ambrosino et al. (KLOE Collaboration), Measurement of the pseudoscalar mixing angle and η' gluonium content with KLOE detector, Phys. Lett. B **648**, 267 (2007).

[12] H. W. Ke, X. Q. Li, and Z. T. Wei, Determining the $\eta - \eta'$ mixing by the newly measured BR$(D(D_s) \to \eta(\eta') + \bar{l} + \nu_l$, Eur. Phys. J. C **69**, 133 (2010).

[13] A. R. Williamson and J. Zupan, Two body B decays with isosinglet final states in SCET, Phys. Rev. D **74**, 014003 (2006).

[14] R. Fleischer, R. Knegjens, and G. Ricciardi, Exploring CP violation and η-η' mixing with the $B_{s,d}^0 \to J/\psi\eta^{(\prime)}$ systems, Eur. Phys. J. C **71**, 1798 (2011).

[15] T. Feldmann, Quark structure of pseudoscalar mesons, Int. J. Mod. Phys. A **15**, 159 (2000).

[16] R. Zhu, Y. Ma, X. L. Han, and Z. J. Xiao, Form factors for semileptonic B_c decays into $\eta^{(\prime)}$ and glueballs, Phys. Rev. D **98**, 114035 (2018).

[17] C. Di Donato, G. Ricciardi, and I. Bigi, $\eta - \eta'$ mixing—From electromagnetic transitions to weak decays of charm and beauty hadrons, Phys. Rev. D **85**, 013016 (2012).

[18] R. L. Workman et al. (Particle Data Group), Review of particle physics, Prog. Theor. Exp. Phys. **2022**, 083C01 (2022).

[19] M. R. Ahmady and E. Kou, Possible large direct CP asymmetry in hadronic $B^{\pm} \to \pi^{\pm}\eta'$ decays, Phys. Rev. D **59**, 054014 (1999).

[20] D. s. Du, C. S. Kim, and Y. d. Yang, A new mechanism for $B^{\pm} \to \eta' K^{\pm}$ in perturbative QCD, Phys. Lett. B **426**, 133 (1998).

[21] I. E. Halperin and A. Zhitnitsky, $B \to K\eta'$ decay as unique probe of η' meson, Phys. Rev. D **56**, 7247 (1997).

[22] A. A. Petrov, Intrinsic charm of light mesons and CP violation in heavy quark decay, Phys. Rev. D **58**, 054004 (1998).

[23] S. Khalil and E. Kou, A Possible Supersymmetric Solution to the Discrepancy between $B \to \phi K_s$ and $B \to \eta' K_s$ CP Asymmetries, Phys. Rev. Lett. **91**, 241602 (2003).

[24] M. Z. Yang and Y. D. Yang, Revisiting charmless two-body B decays involving η' and η, Nucl. Phys. **B609**, 469 (2001).

[25] Z. J. Xiao, Z. Q. Zhang, X. Liu, and L. B. Guo, Branching ratios and CP asymmetries of $B \to K\eta^{(\prime)}$ decays in the pQCD approach, Phys. Rev. D **78**, 114001 (2008).

[26] Y. Y. Fan, W. F. Wang, S. Cheng, and Z. J. Xiao, Anatomy of $B \to K\eta^{(\prime)}$ decays in different mixing schemes and effects of next-to-leading order contributions in the perturbative QCD approach, Phys. Rev. D **87**, 094003 (2013).

[27] Y. Y. Charng, T. Kurimoto, and H. n. Li, Gluonic contribution to $B \to \eta'$ form factors, Phys. Rev. D **74**, 074024 (2006); **78**, 059901(E) (2008).

[28] E. Kou and A. I. Sanda, $B \to K\eta'$ decay in perturbative QCD, Phys. Lett. B **525**, 240 (2002).

[29] A. G. Akeroyd, C. H. Chen, and C. Q. Geng, $B \to \eta^{(\prime)}(l^{-}\bar{\nu}_l, l^{+}l^{-}, K, K^{*})$ decays in the quark-flavor mixing scheme, Phys. Rev. D **75**, 054003 (2007).

[30] H. Y. Cheng, H. n. Li, and K. F. Liu, Pseudoscalar glueball mass from $\eta - \eta' - G$ mixing, Phys. Rev. D **79**, 014024 (2009).

[31] X. Liu, H. n. Li, and Z. J. Xiao, Implications on η-η'-glueball mixing from $B_{d/s} \to J/\Psi\eta^{(\prime)}$ decays, Phys. Rev. D **86**, 011501(R) (2012).

[32] R. Aaij et al. (LHCb Collaboration), Evidence for the decay $B^0 \to J/\psi\omega$ and measurement of the relative branching fractions of B_s^0 meson decays to $J/\psi\eta$ and $J/\psi\eta'$, Nucl. Phys. **B867**, 547 (2013).

[33] R. Aaij et al. (LHCb Collaboration), Study of $\eta - \eta'$ mixing from measurement of $B_{(s)}^0 \to J/\psi\eta^{(\prime)}$ decay rates, J. High Energy Phys. 01 (2015) 024.

[34] R. Aaij et al. (LHCb Collaboration), Search for the $\Lambda_b^0 \to \Lambda\eta'$ and $\Lambda_b^0 \to \Lambda\eta$ decays with the LHCb detector, J. High Energy Phys. 09 (2015) 006.

[35] Z. T. Wei, H. W. Ke, and X. Q. Li, Evaluating decay rates and asymmetries of Λ_b into light baryons in LFQM, Phys. Rev. D **80**, 094016 (2009).

[36] J. Zhu, Z. T. Wei, and H. W. Ke, Semileptonic and nonleptonic weak decays of Λ_b^0, Phys. Rev. D **99**, 054020 (2019).

[37] C. Q. Geng, Y. K. Hsiao, Y. H. Lin, and Y. Yu, Study of $\Lambda_b \to \Lambda(\phi, \eta^{(\prime)})$ and $\Lambda_b \to \Lambda K^{+} K^{-}$ decays, Eur. Phys. J. C **76**, 399 (2016).

[38] M. R. Ahmady, C. S. Kim, S. Oh, and C. Yu, Heavy baryonic decays of $\Lambda_b \to \Lambda\eta'$ decays, Phys. Lett. B **598**, 203 (2004).

[39] A. Datta, H. J. Lipkin, and P. J. O'Donnell, Nonstandard $\eta - \eta'$ mixing and the nonleptonic B and Λ_b decays to η and η', Phys. Lett. B **544**, 145 (2002).

[40] J. Schechter, A. Subbaraman, and H. Weigel, Effective hadron dynamics: From meson masses to the proton spin puzzle, Phys. Rev. D **48**, 339 (1993).

[41] R. Escribano and J. M. Frere, Study of the $\eta - \eta'$ system in the two mixing angle scheme, J. High Energy Phys. 06 (2005) 029.

[42] A. Bramon, R. Escribano, and M. D. Scadron, The $\eta - \eta'$ mixing angle revisited, Eur. Phys. J. C **7**, 271 (1999).

[43] D. J. Gross, S. B. Treiman, and F. Wilczek, Light-quark masses and isospin violation, Phys. Rev. D **19,** 2188 (1979).

[44] D. Gusbin, $\pi^0\eta\eta'$ mixing effects in $K^+ \to \pi^+\pi^0$ decay, Phys. Rev. D **24,** 797 (1981).

[45] W. Qian and B. Q. Ma, Tri-meson-mixing of π-η-η' and ρ-ω-ϕ in the light-cone quark model, Eur. Phys. J. C **65,** 457 (2010).

[46] T. Peng and B. Q. Ma, Tetramixing of vector and pseudoscalar mesons: A source of intrinsic quarks, Phys. Rev. D **84,** 034003 (2011).

[47] P. Ball, V. M. Braun, and E. Gardi, Distribution amplitudes of the Λ_b baryon in QCD, Phys. Lett. B **665,** 197 (2008).

[48] A. Ali, C. Hambrock, and A. Y. Parkhomenko, Light-cone wave functions of heavy baryons, Theor. Math. Phys. **170,** 2 (2012).

[49] G. Bell, T. Feldmann, Y. M. Wang, and M. W. Y. Yip, Light-cone distribution amplitudes for heavy-quark hadrons, J. High Energy Phys. 11 (2013) 191.

[50] Y. M. Wang and Y. L. Shen, Perturbative corrections to $\Lambda_b \to \Lambda$ form factors from QCD light-cone sum rules, J. High Energy Phys. 02 (2016) 179.

[51] A. Ali, C. Hambrock, A. Y. Parkhomenko, and W. Wang, Light-cone distribution amplitudes of the ground state bottom baryons in HQET, Eur. Phys. J. C **73,** 2302 (2013).

[52] V. M. Braun, S. E. Derkachov, and A. N. Manashov, Integrability of the evolution equations for heavy-light baryon distribution amplitudes, Phys. Lett. B **738,** 334 (2014).

[53] V. L. Chernyak, A. A. Ogloblin, and I. R. Zhitnitsky, Wave functions of octet baryons, Z. Phys. C **42,** 569 (1989).

[54] Y. L. Liu, C. Y. Cui, and M. Q. Huang, Higher order light-cone distribution amplitudes of the Λ baryon, Eur. Phys. J. C **74,** 3041 (2014).

[55] Y. L. Liu and M. Q. Huang, Distribution amplitudes of Σ and Λ and their electromagnetic form factors, Nucl. Phys. **A821,** 80 (2009).

[56] G. S. Bali, V. M. Braun, M. Göckeler, M. Gruber, F. Hutzler, A. Schäfer, R. W. Schiel, J. Simeth, W. Söldner, A. Sternbeck *et al.*, Light-cone distribution amplitudes of the baryon octet, J. High Energy Phys. 02 (2016) 070.

[57] V. M. Braun, S. Collins, B. Gläßle, M. Göckeler, A. Schäfer, R. W. Schiel, W. Söldner, A. Sternbeck, and P. Wein, Light-cone distribution amplitudes of the nucleon and negative parity nucleon resonances from lattice QCD, Phys. Rev. D **89,** 094511 (2014).

[58] G. S. Bali *et al.* (RQCD Collaboration), Light-cone distribution amplitudes of octet baryons from lattice QCD, Eur. Phys. J. A **55,** 116 (2019).

[59] Z. Rui, C. Q. Zhang, J. M. Li, and M. K. Jia, Investigating the color-suppressed decays $\Lambda_b \to \Lambda\psi$ in the perturbative QCD approach, Phys. Rev. D **106,** 053005 (2022).

[60] Z. Rui, J. M. Li, and C. Q. Zhang, Estimates of exchange topological contributions and *CP*-violating observables in $\Lambda_b \to \Lambda\phi$ decay, Phys. Rev. D **107,** 053009 (2023).

[61] J. J. Han, Y. Li, H. n. Li, Y. L. Shen, Z. J. Xiao, and F. S. Yu, $\Lambda_b \to p$ transition form factors in perturbative QCD, Eur. Phys. J. C **82,** 686 (2022).

[62] C. H. Chen and H. N. Li, Nonfactorizable contributions to B meson decays into charmonia, Phys. Rev. D **71,** 114008 (2005).

[63] Z. Rui, H. Li, G. x. Wang, and Y. Xiao, Semileptonic decays of B_c meson to S-wave charmonium states in the perturbative QCD approach, Eur. Phys. J. C **76,** 564 (2016).

[64] P. Ball and R. Zwicky, New results on $B \to \pi, K, \eta$ decay form factors from light-cone sum rules, Phys. Rev. D **71,** 014015 (2005).

[65] J. F. Sun, D. S. Du, and Y. L. Yang, Study of $B_c \to J/\psi\pi$, $\eta_c\pi$ decays with perturbative QCD approach, Eur. Phys. J. C **60,** 107 (2009).

[66] P. Ball and G. W. Jones, $B \to \eta^{(\prime)}$ form factors in QCD, J. High Energy Phys. 08 (2007) 025.

[67] C. H. Chou, H. H. Shih, S. C. Lee, and H. n. Li, $\Lambda_b \to \Lambda J/\psi$ decay in perturbative QCD, Phys. Rev. D **65,** 074030 (2002).

[68] H. H. Shih, S. C. Lee, and H. n. Li, The $\Lambda_b \to pl\bar{\nu}$ decay in perturbative QCD, Phys. Rev. D **59,** 094014 (1999).

[69] H. H. Shih, S. C. Lee, and H. n. Li, Applicability of perturbative QCD to $\Lambda_b \to \Lambda_c$ decays, Phys. Rev. D **61,** 114002 (2000).

[70] H. H. Shih, S. C. Lee, and H. N. Li, Asymmetry parameter in the polarized $\Lambda_b \to \Lambda_c l\bar{\nu}$ decay, Chin. J. Phys. **39,** 328 (2001).

[71] X. G. He, T. Li, X. Q. Li, and Y. M. Wang, PQCD calculation for $\Lambda_b \to \Lambda\gamma$ in the standard model, Phys. Rev. D **74,** 034026 (2006).

[72] C. D. Lu, Y. M. Wang, H. Zou, A. Ali, and G. Kramer, Anatomy of the pQCD approach to the baryonic decays $\Lambda_b \to p\pi, pK$, Phys. Rev. D **80,** 034011 (2009).

[73] C. Q. Zhang, J. M. Li, M. K. Jia, and Z. Rui, Nonleptonic two-body decays of $\Lambda_b \to \Lambda_c\pi, \Lambda_c K$ in the perturbative QCD approach, Phys. Rev. D **105,** 073005 (2022).

[74] G. Buchalla, A. J. Buras, and M. E. Lautenbacher, Weak decays beyond leading logarithms, Rev. Mod. Phys. **68,** 1125 (1996).

[75] H. Y. Cheng, Nonleptonic weak decays of bottom baryons, Phys. Rev. D **56,** 2799 (1997); **99,** 079901(E) (2019).

[76] P. Ball, V. M. Braun, and A. Lenz, Higher-twist distribution amplitudes of the K meson in QCD, J. High Energy Phys. 05 (2006) 004.

[77] J. F. Hsu, Y. Y. Charng, and H. n. Li, Okubo-Zweig-Iizuka-rule violation and $B \to \eta^{(\prime)}K$ branching ratios, Phys. Rev. D **78,** 014020 (2008).

[78] Y. K. Hsiao, Y. Yao, and C. Q. Geng, Charmless two-body anti-triplet *b*-baryon decays, Phys. Rev. D **95,** 093001 (2017).

[79] Y. K. Hsiao, P. Y. Lin, C. C. Lih, and C. Q. Geng, Charmful two-body anti-triplet *b*-baryon decays, Phys. Rev. D **92,** 114013 (2015).